Validation of NO_2 column densities around different cities of Pakistan by using various instruments.

By

M.SHEHZAIB ANJUM ALI

(00000273374)

A thesis submitted in partial fulfillment of the requirements for the degree of Master of

Science in Environmental Science

Institute of Environmental Sciences and Engineering,

School of Civil and Environmental Engineering,

National University of Sciences and Technology

Islamabad, Pakistan

(2021)

THESIS ACCEPTANCE CERTIFICATE

It is certified that the contents and forms of the thesis entitled **"Validation of NO_2 column densities around different cities of Pakistan by using various instruments"** submitted by **Mr. Muhammad Shehzaib Anjum Ali**, Registration No. **00000273374** has been found satisfactory for the requirements of the degree of Master of Science in Environmental Science.

Supervisor: _____
Dr. Muhammad Fahim Khokhar
Professor
IESE, SCEE, NUST

Head of Department: _____
Dr. Muhammad Fahim Khokhar
IESE, SCEE, NUST

Dean/Principal: _____
SCEE, NUST

CERTIFICATE

It is certified that the contents and forms of the thesis entitled **"Monitoring of NO_2 column densities around different cities of Pakistan by using various instruments"** submitted by Mr. Muhammad Shehzaib Anjum Ali has been found satisfactory for the requirements of the degree of Master of Science in Environmental Science.

Supervisor: _____
Dr. Fahim Khokhar
Professor
IESE, SCEE, NUST

Member:

_____
Dr. Muhammad Arshad
Associate Professor
IESE-SCEE, NUST

Member:

_____
Dr. Zeeshan Ali Khan
Associate Professor
IESE-SCEE, NUST

I dedicate this thesis to my beloved parents and siblings who have been a source of inspiration for me throughout my life.

ACKNOWLEDGEMENT

First and foremost, I acknowledge that it is by the grace of **Almighty Allah** that I have been able to complete this manuscript. All respect to the **Holy Prophet (P.B.U.H)** whose life is the model I have based my life around.

Next, I express my utmost thanks to my supervisor **Professor Dr. Fahim Khokhar**, who has supported and guided me throughout my research. His keen interest and valuable suggestions have helped my overcome any and all obstacles encountered during my research work. I will forever be thankful for his incredible guidance, encouragement, and sympathetic attitude during the entire period of my research. I am also thankful for the meaningful advice and inspiring attitudes of **Dr. Zeeshan Ali Khan** and **Dr. Muhammad Arshad** which encouraged me to work harder during my research.

This acknowledgement would be incomplete if I do not pay my sincere and heartedly thanks to my cherished and loving parents for their sacrifices, prayers, and affections without which it would have been nearly impossible to achieve my goals. My sincerest thanks to all my friends at IESE and other institutes for their continuous support and encouragement throughout my time at NUST. Last but not the least I would like to thank all the laboratory staff at IESE for their help and cooperation.

M. Shehzaib Anjum Ali

TABLE OF CONTENTS

LIST OF ABBREVIATIONS

AMF	Air Mass Factor
ArcGIS	Arc Geographic Information System
DOAS	Differential Optical Absorption Spectroscopy
DOASIS	Differential Optical Absorption Spectroscopy Intelligent System
DSCD	Differential Slant Column Densities
FTIR	Fourier Transform Infrared Spectrometry
FWHM	Full Width Half Maximum
HNO_3	Nitric Acid
JICA	Japan International Cooperation Agency
MAX-DOAS	Multi-axis Differential Optical Absorption Spectroscopy
NDIR	Non-Dispersive Infra-Red
NO	Nitric Oxide
NO_2	Nitrogen Dioxide
NO_2 SCD	Nitrogen Dioxide Slant Column Density
NO_2 VCD	Nitrogen Dioxide Vertical Column Density
NO_2^-	Nitrites
NO_3^-	Nitrates
NOx	Oxides of Nitrogen
O_3	Ozone
OMI	Ozone Monitoring Instrument
OSHA	Occupational Safety & Health Administration

Pak-EPA	Pakistan Environmental Protection Agency
Pak-NEQs	Pakistan National Environmental Quality Standards
PAN	Peroxy Acetyl Nitrile
PM	Particulate Matter
USEPA	United States Environmental Protection Agency
UTC	Coordinated Universal Time
UV	Ultra-Violet
VOCs	Volatile Organic Compounds
WHO	World Health Organization
WinDOAS	Windows Differential Optical Absorption Spectroscopy
ppb	Parts per Billion
RMS	Root Mean Square
OMI	Ozone Monitoring Instrument
VOCs	Volatile Organic Compounds
RMS	Root Mean Square

LIST OF TABLES

List of Figures

ABSTRACT

Air pollution has emerged as a major environmental challenge with sever impacts on health and functioning of human society. In recent years, the intensity of its impacts has become more and more pronounced, most notably in developing countries such as Pakistan which lacks adequate monitoring, protection, and management systems. Epidemiological studies have linked poor air quality conditions with different health disorders and increasing mortality rates. In Pakistan, the annual burden of disease from outdoor air pollution has been estimated to be responsible for around 22,000 premature adult deaths and the loss of around 163,432 DALY. (disability-adjusted life years). The concentration of major air pollutants in Pakistan such as NOx, O_3 and SO_2 have increased significantly over the last two decades. Multiple studies have also reported poor air quality in the major cities of Pakistan exceeding the national guidelines. However, because of the lack of regular ground-based monitoring and absence of baseline studies, the situation in various cities of the country is still largely unknown. This study aims to address that knowledge gap, through detailed assessment of a prominent criteria pollutant (NO_2) across various cities of Pakistan. Various ground and satellite-based observations have been used throughout this study and their results have been validated through inter-comparisons.

The cities focused on during this study were: Islamabad, Lahore and Multan. Since 2015 regular ground-based monitoring of NO_2, has been carried out at IESE-NUST using Multi-Axis Differential Optical Absorption Spectroscopy (MAX-DOAS). The results of these analysis have been compared with tropospheric satellite measurements taken from OMI (available since 2004) and TROPOMI (available since 2018). A similar trend has been observed for the daily NO_2 column densities across all three instruments, and correlation of MAXDOAS observations between TROPOMI and OMI being 0.80 and 0.77 for daily values and 0.90 and 0.80 for monthly averages, respectively. NO_2 diurnal variations were noticed with high concentrations during low sunlight and heavy traffic loads. Seasonal variation in satellite observations also showed an increasing trend in NO_2 concentrations with both OMI and TROPOMI, showing a significant increase after 2009.

The study in Lahore and Multan involved ground-based analysis supplemented with monthly field campaigns. Different meteorological parameters were compared with daily visibility incidences to understand the impact of yearly smog episodes. According to the comparisons, visibility incidences (prominently those observed in Lahore) from 2016 onwards have exhibited a temporal shift with their onset being moved back by around one week. The role of agriculture burning activities across both sides of the border were also assessed using MODIS fire counts and $PM_{2.5}$

data from US embassy's located in Lahore and Delhi. Results show that agricultural fire activities are at their maximum intensity during a 20-day period from October-25 to November-14. The $PM_{2.5}$ concentrations also show a significant increase during this time, indicating the impact of seasonal fire activities on air quality on both sides of the international border.

Finally, Car-MAXDOAS-field campaigns were conducted to determine the potential sources of pollution within the cities of Lahore and Multan. These field campaigns revealed that major sources of NO_2 pollution in Lahore were vehicular emissions and industrial emissions, and wind-currents can carry this pollution down-stream from its sources. The potential transboundary impacts on air quality in Lahore were also calculated using back-trajectory analysis in conjunction with MAX-DOAS. And transboundary emissions in Lahore can account for around 30% of the NO_2 pollution. Finally, NO_2, NO and NOx observations carried out at GCU-Lahore and BZU-Multan sites revealed that ambient concentrations routinely exceed prescribed limits and, therefore, air quality in both cities is of growing concern.

Chapter 1

1. INTRODUCTION

1.1. Background

Air pollution as defined by the US EPA refers to the presence of contaminating substances in the atmosphere that interfere with human health and welfare and produce a variety of harmful environmental effects. The annual worldwide consequences of air pollution range from reduced life expectancy (of millions), damage to crops which can feed millions and increased climatic disturbances which can costs millions $. As a result of these negative consequences of air pollution i.e., climate change, increased mortality and morbidity, its position as one of this era's greatest challenges has become clear. However, because the majority of its impacts are distributed unevenly and often poorly understood, finding adequate solutions for this problem has proven to be difficult (Manisalidis et al., 2020).

Out of all the world's known air pollutants, the six criteria pollutants (NOx, SO2, Tropospheric O3, CO, PM, Pd) account for most of the world's air pollution and their linkage with several different health effects has led to the development of various ambient air quality standards around the globe. In Pakistan, ambient air quality standards as well as other tangible limits on the emissions of these pollutants have also been prescribed in the national and provincial levels. However due to the lack of monitoring infrastructure and absence of long-term, studies the situation of these criteria pollutants in Pakistan has remained a mystery.

The major goal of this study is to determine the concentration of one of these criteria pollutants (NO_2); formed as the consequence of fossil fuel consumption and industrial activities, in some of the major cities of Pakistan using various ground-based instruments such as MAX-DOAS, HAZ-Scanners and validation of these ground-based results using satellite observations.

Nitrogen dioxide (NO_2) is produced from both natural and anthropogenic processes. Prolonged exposure to this pollutant, has been associated with a wide variety of severe health impacts such as hypertension, various cardiovascular disease, diabetes and even death (Ogen, 2020). Nitrogen oxides (NOx) can also cause deterioration of environmental health in various ways. Such as through the destruction of the ozone layer, production of Photochemical smog and contribution towards acid rain. Additionally, breakdown of NO_2 and its oxides can result in the production of secondary products such as O_3 and $PM_{2.5}$.

Major sources of air pollution in Pakistan include huge quantities of emissions from motor vehicles and medium and small-scale industries which have steadily increased, from 2006-2019 the number of registered vehicles in the country have increased by 400% (Khwaja & Khan, 2005; PES, 2019.). From 2016 onwards, the number of annual periodic smog episodes in the country have increased significantly, smog is now considered a fifth season in the country and its annual impacts include disruptions in socio-economic activities and poor health impacts which can be felt around the various cities of the country. Figure 1.1. Highlights prevalent conditions of smog throughout various cities of Punjab, Pakistan.

Figure 1. 1: Winter smog across various cities of Pakistan

From the year 2016 onwards, the onset of smog has been observed during the first week of November. These smog episodes are primarily driven by agricultural fire activities (mostly rice paddy burning, taking place at the Indian side of Punjab), but a significant contribution is believed to be from local sources.

Temperature and solar radiation are also important factors as they affect the type and rate of the atmospheric chemical reactions; resultantly, they play an important role in photochemical smog and/or secondary aerosols formation. Relative humidity distribution is one of the important parameters that can alter the environmental temperature. The high levels of relative humidity result from an increased number of water vapors; consequently, more fog formation. The existence of high humidity in the air with chemical pollutants and aerosol plays an important role in smog formation (Mohammadi et al., 2012).

1.2. Study site

The Eastern plains of Punjab, Pakistan are densely populated and host most of the agricultural activities. It is evident from Figure 1.2 that most of these areas are afflicted by an intense layer of aerosols during the winter months. In order to cover the maximum spatial extent and north-south gradient (climatic conditions), two major cities of Lahore and Multan are selected for field activities as shown in Figure 1.3:

Figure 1. 2: Winter smog over South-Asia, observed through satellite observations.

Site #1: Islamabad, is the capital of Pakistan (lat: 33.6844° N, lon:73.0479° E-with over 1 million inhabitants), the study site was IESE, NUST. Major sources of pollution included the busy Srinagar highway and I9 industrial area. The study site will be referred to as ISB-Site in this study.

Site #2: Lahore is the 2nd most populous city (lat:31°32′59″N, lon:74°20′37″E - with more than 10 million inhabitants) and hosts various types of industries including power generation, textile, pharmaceutical, steel manufacturing, foundries, and a huge number of cottage industry. The Govt. College University (GCU) campus Lahore was chosen for various measurements and is referred to as LHR-Site in this study.

Site#3: Multan is the fifth most populous city (lat: 30°11′52″N, lon: 71°28′11″E, inhabitants are about 1.2 million) in Pakistan. The highest recorded temperature in the city is approximately 52 °C, whereas the lowest recorded temperature is approximately −1 °C. Dust storms are a common occurrence in this region. Monitoring set up was established at the Baha Uddin Zakariya University Campus, Multan, and is referred to as MTN-Site in this study.

Figure 1. 3: Monitoring sites in Pakistan

Chapter 2

2. LITERATURE REVIEW

2.1. The Earth's Atmosphere

Atmosphere is defined as the layer of gases surrounding the earth it is responsible for sustaining life by, providing air (O_2) for respiration, regulating the planets various climate systems and absorbing harmful UV radiations coming from the sun. It is generally composed of a layer of various gases which present in specific concentrations make sustaining life possible.

2.2. Structure of the Atmosphere

The planet's atmosphere is sub-divided into four layers: the troposphere that houses all life near the surface of the earth; the stratosphere which exists above the troposphere and contains the ozone layer; the mesosphere, above the stratosphere and a colder and less dense layer composing around 0.1% of the atmosphere; the thermosphere, the top layer, with high temperatures and low molecular density. There extent of the gaseous envelop around the planet is categorized as the "final frontier" or exosphere. There are also transitionary layers which exist between and sperate the beforementioned layers, the transitionary layers are: the tropopause sandwiched between the troposphere and stratosphere; the stratopause existing between the stratosphere and mesosphere and the mesopause existing between mesosphere and thermosphere.

2.2.1. Troposphere

It is the lowest part of the atmosphere; it exists close to the surface and drives the weather system of the planet. In terms of mass, most of the atmosphere is contained within this layer. Th height of the troposphere varies according to the temperature and location. However,

generally Its thickness is between 7 to 8 km at the poles and 16 to 18 km at the equator. This geographic variation is because of the rotation of earth which tends to shift air masses towards the equator. Also because of the variation in insolation between the equator and the poles, the temperature at the equator is always higher. Temperature in the troposphere generally decreases with height leading to the phenomenon of convection currents and weather patterns with drive climate systems throughout the earth (Holton et al., 1995).

2.2.2. Stratosphere

Above the troposphere is the stratosphere, a layer extending around 50 km vertically and separated from the troposphere through the tropopause. It is the second major layer of the atmosphere, comprising 15% of the mass of the atmosphere. No weather exists in the stratosphere, and hence because of the atmospheric stability and incident solar radiation the ozone layer exists within this layer. The ozone layer blocks harmful short-wave UV radiation coming from the sun that if exposed to the surface can lead to harmful health affects like cancer and skin diseases. Without the ozone layer, it would be impossible for life to exist on this planet. The process of ozone formation in the stratosphere leads to higher temperatures in the stratosphere, and as a result temperature increases with altitude (Brasseur & Solomon, 2006; Holton et al., 1995).

2.2.3. Mesosphere

Above the stratosphere and below the thermosphere exists the mesosphere, the third layer of the atmosphere. The height of this layer extends up to 80 km above the surface of the earth. Throughout the mesosphere, temperature decreases with height. The coldest temperatures in the Earth's atmosphere, about -90°C are found near the top of this layer. This layer is also important as it protects the earth from incoming meteors by burning them through friction (Roble, Experiment, & Theory, 1995). The temperature decreases with increasing altitude in this layer. Since most of the meteors vaporize in the mesosphere, some of their materials linger

and thus this layer has a relatively high concentration of iron and other metals. Around the poles, some peculiar high-altitude clouds sometimes form called “polar mesospheric” clouds or “noctilucent” clouds. These strange clouds are formed much, much higher than any other type of cloud. Because of the temperature any water vapors which enter the mesosphere are frozen hence like the stratosphere this layer is very dry, a fact which makes the formation of clouds that much more surprising. Strange electrical discharges like lightning are also occasionally observed in the mesosphere. The stratosphere and mesosphere are sometimes called the middle of the atmosphere. At the mesopause and below gases composed of different types of atoms and molecules are thoroughly mixed by turbulence in the atmosphere. Whereas above the mesosphere i.e., in the thermosphere and above, the collision of gas particles is so infrequent that the gases separate based on their types of chemical elements.

2.2.4. Thermosphere

Above the mesosphere, lies the thermosphere which extends from 85 km to 600 km above the earth’s surface. Most telecommunication satellites orbit in this layer and here temperature increases with altitude. Temperature increase is mostly a result of the relative stability and high solar activity within this layer. In this layer UV radiations are responsible for the creation of ions through the photoionization of molecules (Lübken, 1999).

2.3. Air Pollution

Air pollution is the presence of any contaminants that can overwhelm the natural cleaning capacity of the atmosphere and results in changes to natural processes and cause adverse effects to the environment (Cerbu et al., 2019). Through various anthropogenic and natural process, atmospheric pollutants are released into the environment which can not only cause disruptions to natural cycles but also result in various adverse health effects on humans. The health and environmental impacts of atmospheric pollutants such as Nitrogen oxides (NO,NO_2), Ozone (O_3) and Particulate Matter (PM_{10} and $PM_{2.5}$) differ with respect to their composition,

reactivity, spatial and temporal distributions, and decomposition (Gaffney & Marley, 2003; Gheorghe & Ion, 2011; Kasuga, 1989).

Exposure to such pollutants results in serious health effects which can range from cancer to other respiratory disorder. Recent year studies have linked the air pollution with increased mortality and reduced life expectancy (Bonyadi et al., 2020; Gowers et al., 2020; Lelieveld et al., 2020; Seposo et al., 2020; Yin et al., 2020).

2.4. A major criteria Pollutant: NO_2 (Nitrogen Dioxide)

Criteria pollutants are a set of pollutants that were first highlighted by United States Environment Protection Agency for the need of regulation because of their hazardous effects on human and environment in the form of acid rain, smog and other health related issues. Today, these are used to identify the quality of air.

Nitrogen dioxide (NO_2) is a brownish colored gas with a pungent irritating smell, released primarily from combustion and industrial activities. Occasionally, it is seen as a brown haze over traffic congested major cities. NO_2 is a major criteria pollutant that has been difficult to control since the beginning, it released from a wide-variety of sources such as: automobiles, industries, power-generation, lightning, and combustion. With the rapid growth in the world's population in recent years, there has been a dramatic increase in these sources, such as the rise in motor-vehicles, rampant industrialization etc. which have resulted in the concentration of NO_2 and its status as a major air pollutant rising around Pakistan. (ul-Haq et al., 2014, 2017; Ul-Haq et al., 2015; Zeb et al., 2019)

Pakistan National Environmental Quality Standard, 2010 has suggested 80 $\mu g/m^3$ of NO_2 as a limit for prevention of sensory irritation in population, for 24 hours.

NO2 is a pollutant in both the troposphere and stratosphere, and hence plays an important role in the chemistry of both spheres. In the stratosphere, it actively takes part in the ozone

destruction cycle and the conversion of Halogen Oxides (O-X) into much less reactive species. While, in troposphere, it is involved in ozone formation and is a potential precursor for smog and acid rain-formation. It also plays a role in global warming through radiative forcing in the atmosphere.

2.5. Sources of NO_2

Globally, NO_2 production is driven primarily by human activities, as higher concentrations of this pollutant are found in the northern hemisphere, specifically around heavily populated areas with busy urban centers. Anthropogenic activities, such as fossil fuel combustion provide favorable conditions for the release of NOx into the atmosphere. Because of the relatively short lifetime of NO_2 in the atmosphere there is still a high degree of uncertainty with respect to its emission sources. Nevertheless, the transport sector is still considered as the major emission source of NO_2 in atmosphere (Chen et al., 2020; Lu et al., 2020).

Natural sources of NOx include forest fires, lightning and soil emission driven by microbial activities (Ibrahim, 2009). Naturally produced methane reacts with $OH^{\cdot}$ radicals to produce peroxy radicals, these radicals oxidize nitric oxide into NO_2 (Nakazawa & Taroh Matsuno, 2020; Vestin et al., 2020)

2.6. Measurement Techniques for NO_2

As mentioned above, NO_2 is an important precursor for tropospheric ozone formation and therefore the ability to make unequivocal measurements of its concentrations, with respect to the concentrations of other precursors such as VOCs and oxidizing radicals such as (H2O2) can help significantly improve our understanding of tropospheric ozone formation and pollution. In order for measurements to be meaningful, reliable instruments and techniques must be utilized. As the estimates provided by these instruments are the benchmarks against which our theoretical understanding of atmospheric chemistry is tested, the relative uncertainty

in measurements must be adequately known. The benefits of having meaningful estimates of atmospheric trace gases include opportunities for comparing theory and observations; the ability to reliably merge results from separate studies into gradients of observations over large distances with comparable time-periods. For e.g. if reliable and robust monitoring network is in place then seasonal patterns and spatial differences can be more easily measured. The ability to accurately assess the atmospheric composition of a pollutant, combined with adequate theoretical understanding can help provide the ability to test the reliability of control measures in regulating the emission of anthropogenic oxidant precursors and effectively curbing the concentration of these compounds on the environment (NRC, 1992). For the accurate measurement of NO_2 in the atmosphere, the following techniques are available.

2.6.1. Chemiluminescence Methods

The chemiluminescent technique is widely used for continuous monitoring of NO_2 concentrations throughout the world. Chemiluminescence refers to the process of fluorescence occurring during a chemical reaction. For the measurement of NO_2, the instrument measures the reaction of NO with O_3 which produces an excited form of NO2. When the excited NO_2 molecule its returned to its ground state a characteristic fluorescent radiation is emitted, the intensity of which is proportional to the concentration of NO.

$NO + O3 \rightarrow NO_2^* + O2$ $NO_2^* \rightarrow NO_2 + hv$ (Equation 1)

Where hv represents the emitted radiation.

It is important to understand that chemiluminescent analyzers do not measure NO_2 concentrations directly. It measures the concentrations indirectly, by first converting the NO2 component of visible air sample into NO (Through NO2 to NO converter) and then after obtaining total concentration of NOx, subtracting NO:

$NO2 = NOx - NO$ (Equation 2)

Because of this indirect method, the instrument needs to make two independent measurements, of NO and NOx (NO+NO2). This can be achieved through a dual-chamber configuration that measures NOx and NO simultaneously although in different reaction chambers (Defra, 2002).

2.6.2. Electrochemical Sensor

Electrochemical sensors are portable, cost effective sensors used to measure the concentration of trace gases in ambient air. Because of their high sensitivity, low costs and long sample retention time these sensors are ranked among the best of all NO_2 sampling techniques. The instrument's working is based on the electrochemical reduction of NO_2 between electrodes, dipped in electrolyte. The NO_2 contained in the sample makes way into the reaction chamber of cell through diffusion, where it is reduced at the electrode. Because of this reduction a potential difference is created, which produces current proportional to the concentration of NO_2 in the sample. These instruments can be used to find NO2 concentrations in ambient air directly and are used in studying exposures from an occupational health and safety perspective.

2.6.3. Passive Samplers

Diffusive passive samplers for NO_2 are simple inexpensive devices that have been used for the measurement of ambient NO2 concentrations since many years. Widely used samplers are based around a design introduced by Palmes (Palmes et al., 1976) and are comprised of an acrylic tube/ or some other substance that can be sealed at both ends. At one end of the tube, there is a stainless steel grid coated with triethanolamine that adsorbs NO_2 to produce a nitrite salt, which can be used to determine the concentration of NO_2 by colorimetry (Defra, 2002).

2.6.4. Satellite Remote Sensing

The importance of satellite observations as effective tools for qualitative and quantitative evaluation of the distribution of several atmospheric gases have been cited by various studies (Beirle et al, 2003; Martin, 2008, Burrows, Platt, & Borrell, 2011; Lee et al., 2011; Lin,

McElroy, & Physics, 2011; Fioletov et al., 2013). Although satellite observations have limitations such as coarse resolutions, coarse spatial resolutions, intermittent observations, and requiring frequent ground-based validation to improve the accuracy of retrieved information. But marked improvements have been seen, the TROPOspheric Monitoring Instrument (TROPOMI) has been launched aboard the sentinel 5P satellite and because of its high spatial resolution it is able to detect local NO_2 pollution more clearly then its predecessors such as OMI, GOME, GOME-2 and SCIAMACHY.

2.6.5. Spectroscopic Method (DOAS)

In Pakistan, the annually recurring and much publicized smog episodes, observed in many urban regions of Punjab are considered evidence of poor air quality in the country. However, much information about these smog episodes is still limited, such as the impacts of local and transboundary emissions. Air is not limited by borders, and prevailing winds from polluted regions might be responsible for compromising the air quality in other regions, whereas meteorological dynamics such as boundary layer heights may be responsible for exasperating the situation further.

All of the measurement techniques mentioned above must be conducted in designated monitoring sites or near point sources, such as congested intersections etc. Consequently, when using these techniques, the local spatial variability of pollutant as well as the role of boundary layer dynamics is largely neglected.

Multi-axis differential optical absorption spectroscopy (MAX-DOAS) is a relatively new technique, designed to measure NO_2 concentrations with respect to boundary layer information and diurnal profiles (Hönninger et al., 2004). This technique utilizes the principle of remote sensing to compare the intensity of scattered light measured in real-time at different elevation

and azimuth angles. It relies on the narrowband absorbance of atmospheric pollutants within the UV and visible ranges and estimates the vertical and horizontal profiles of the pollutant.

MAXDOAS observations draw upon the advantages of both point and satellite based measurements, they provide pollution concentrations covering a horizontal resolution between 3-15 km (lower-troposphere), with good temporal resolutions (around 1 minute) (Irie et al., 2011; Heckel et al., 2005). Another advantage of this technique is that the same instrument can be used to measure several trace gases simultaneously using the same basic principle, which helps save time and allows for analysis of different components of observed air masses. Currently, the versatility of the MAX-DOAS technique has been further enhanced by using it to take field measurements, in conjunction with cars, ships, air-crafts etc.

2.7. NO_2 Chemistry in atmosphere

The burning of fossil fuels or high temperature ~3000^oC, break oxygen molecules into single, reactive oxygen atoms which react with the abundant nitrogen molecule already present in the air to produce NO or NO_2 (collectively called NOx). NO_2 breaks down rapidly into NO in the presence of UV radiation *(λ < 420 nm). NO* is also produced by the reaction of naturally produced methane with hydroxy ions. The nitrogen oxides can be deposited to the surface through wet-deposition during rain (acid-rain), NO_2 in this situation mixes with water to produce HNO_3 (Guenther et al., 2000).

A comparatively stable compound nitrogen peroxide is also produced by microbial activity, this can diffuse into the stratosphere and because of the high energy short-wave radiation (λ *=185- 230 nm*) degrade into N_2 and O atom. This oxygen atom can then once again reacts with N_2 to form NO which can be converted NO_2 in the presence of O_3.

During the daytime, the interconversion of NO and NO_2 effectively takes place between one minute and is such that the net production of ozone in unaffected, hence this cyclic conversion

is known as the Null cycle. Eq 3, 4 and highlight the null cycle, where nitric oxide reacts with an ozone molecule to produce nitrogen dioxide and an oxygen molecule (eq.3) (Kreher et al., 2019).

$$NO + O_3 \rightarrow NO_2 + O_2 \qquad \text{Eq. 3}$$

The nitrogen dioxide produced breaks down in the presence of UV ($\lambda < 420$ nm) into nitric oxide and an oxygen atom (eq.4).

$$NO_2 + UV\ (\lambda < 420\ nm) \rightarrow NO + O\ (3P) \qquad \text{Eq. 4}$$

This oxygen atom reacts with oxygen molecule to form ozone again (eq. 5).

$$O\ (3P) + O_2 \rightarrow O_3 \qquad \text{Eq. 5}$$

In the absence of UV radiations, this null cycle breaks down with NO_2 reacting with an oxygen atom and producing an oxygen molecule and nitric oxide (eq. 6).

$$NO_2 + O\ (3P) \rightarrow O_2 + NO \qquad \text{Eq. 6}$$

2.8. Impacts of Nitrogen Dioxide

As mentioned before exposure to high concentrations of NO_2 has been reported to cause damage to the respiratory system and cause various other health issues in humans. It also has negative consequences for aquatic and terrestrial ecosystems.

In the atmosphere, the interconversion of NO and NO_2 continuously takes place in a balance called the null cycle. However, because of anthropogenic activities this cycle is disturbed. Large quantities of vehicular and industrial emissions result in large quantities of NO_2 accumulating in urban areas which acts as a precursor to photochemical smog and acid rain (Seangkiatiyuth et al., 2011). Because of the accumulation of NO_2 in urban areas and consequent production of smog societies are adversely affected either because of physical

ailments e.g. irritation and damage to eyes and skin of exposed humans. As well as through disturbances caused to economic activities of the affected area.

2.9. Air quality monitoring studies in Pakistan

Table 1.1: List of the air pollution monitoring studies carried out across Pakistan during last two decades

Study	Location	Monitoring Interval	Specie above WHO standards
(JICA, 2000)	Lahore, Islamabad, and Rawalpindi	April 2000 - May 2000	NO_x and PM_{10}
(Ghauri et al., 2007)	Karachi, Lahore & Quetta	2003-2004	TSP and PM_{10} CO SO_2, NO_X & O_3
(Biswas, et al., 2008)	Lahore	Dec 2005 - Feb 2006	$PM_{2.5}$
(Raja et al., 2010)	Lahore	Nov 2005 - Jan 2006	$PM_{2.5}$
(Lodhi et al., 2009)	Lahore	Nov 2005 - Jan 2006 Feb 2006 -March 2006 Nov 2006 - Dec 2007	$PM_{2.5}$
(Zhang et al., 2008)	Lahore	13 March - 16 April 2006	PM_{10}
(Colbeck et al., 2011b)	Lahore	Nov 2007	PM_1, $PM_{2.5}$, PM_{10} & CO
(Stone et al., 2010)	Lahore	12 Jan 2007 – 19 Jan 2008	$PM_{2.5}$ and PM_{10}
(Khwaja et al., 2012)	Karachi	Aug 2008 – Aug 2009	$PM_{2.5}$
(Sughis et al., 2012)	Schools located in Lahore	12 - 23 Jan 2009	$PM_{2.5}$
(Alam et al., 2011)	Karachi Lahore Rawalpindi Peshawar	March – April 2010	$PM_{2.5}$ and PM_{10}
(Jahangir et al., 2013)	Rawalpindi Islamabad	March – June 2010	NO_2

(Ahmad & Aziz, 2013)	Rawalpindi Islamabad	Nov 2008 – Aug 2010 Sep 2010 – March 2011	NO_2 & O_3
(Zafar et al., 2012)	Rawalpindi Islamabad	Jan – Feb 2011 March – April 2011	NO_2
(Alam et al., 2015)	Peshawar	1 April 2011 – 20 April 2011	$PM_{2.5}$ & PM_{10}
(Javed et al., 2014)	Faisalabad	May 2012	TSP, $PM_{2.5.}$ PM_4 & PM_{10}
(Shabbir et al., 2016)	N-5 Highway (Islamabad to Lahore section)	Nov 2012	NO_2
(Jalees et al., 2016)	Northern Part of Lahore	Dec 2012 – Feb 2013	TSP and trace metals (Fe, Zn, Ni, Pb, Cu, Mn, As, Cr)
(Khokhar et al., 2016b)	Islamabad and Rawalpindi	13 Nov 2012 16 Nov 2012 13 Dec 2013	NO_2
(Niaz et al., 2016)	Faisalabad	Jan – Dec 2013	$PM_{2.5}$ (Average Concentrations)
(Khokhar et al., 2017)	IESE-NUST Islamabad	Feb – March 2013	NO_2

2.10. Pakistan National Environmental Quality Standards

Pakistan Environmental Protection Agency has formulated standards for all the major air pollutants (table 2) to curtail the levels of air pollution in the country. Industries are regulated by these National Environmental Quality Standards (NEQs) for ambient air.

Table 1. 2: List of NEQs for ambient air in Pakistan

Pollutants	Time-Weighted Average	Concentrations in Ambient Air	Method of Measurement
Sulphur Dioxide (SO_2)	Annual Average	80 µg/m³	Ultraviolet Fluorescence Method
	24-Hour Average	120 µg/m³	
Oxides of Nitrogen as (NO)	Annual Average	40 µg/m³	Gas Phase Chemiluminescence
	24-Hour Average	40 µg/m³	
Oxides of Nitrogen as (NO_2)	Annual Average	40 µg/m³	Gas Phase Chemiluminescence
	24-Hour Average	80 µg/m³	
Ozone (O_3)	1-Hour Average	130 µg/m³	Non-Dispersive UV Absorption Method
Suspended Particulate Matter (SPM)	Annual Average	360 µg/m³	High Volume Sampling (Average flow rate not less than 1.1 m3/minute
	24-Hour Average	500 µg/m³	
Respirable Particulate Matter (PM 10)	Annual Average	120 µg/m³	-β Ray Absorption Method
	24-Hour Average	150 µg/m³	
Respirable Particulate Matter (PM 2.5)	Annual Average	15 µg/m³	-β Ray Absorption Method
	24-Hour Average	35 µg/m³	
	1-Hour Average	15 µg/m³	
Lead (Pb)	Annual Average	1 µg/m³	ASS Method after sampling using EPM 2000 or equivalent Filter Paper
	24-Hour Average	1.5 µg/m³	
Carbon Monoxide (CO)	8 Hours Average	5 mg/m³	Non-Dispersive Infrared (NDIR) Method
	1-Hour Average	10 mg/m³	

2.11. Planetary Boundary Layer: Diurnal and Seasonal Trends

As a ground-based remote-sensing technique, MAX-DOAS observations, especially those collected at low elevation angles, are directly influenced by the dynamics of the planetary boundary layer (PBL). This atmospheric region exists in the lower troposphere, typically extending from the ground to a height of 0.5 to 2 km during the day at mid-latitudes (Artiola et. al., 2004; Bauer, 1996). Coincident observations of a decrease in air quality and shallow

PBL have indicated that the depth of the boundary layer directly influences human exposure to pollution, and hence, should be routinely monitored (Chou et. al., 2007). The PBL consists of three components: the surface layer, the mixed layer, and the transition layer. The surface layer, located closest to the Earth, is governed by strong frictional processes and generally accounts for 10% of the PBL depth (Garratt, 1992; Bauer, 1996). The mixed layer is located above the surface layer, and is subject to turbulent mixing. Above the mixed layer is the entrainment zone, acting as a transition region between the convective mixing that occurs below it, and the relatively stable air mass of the free troposphere located above the PBL. The terrestrial mixing layer undergoes a diurnal cycle, with a growing convective mixing layer in the morning, and simultaneous decay of the previous day's residual boundary layer, due to an increasing sensible heat flux (W/m^2). Atmospheric instability, induced by the positive gradient between atmospheric and adiabatic lapse rate maintains turbulence within the boundary layer. Under cloud-free conditions, the mixing layer is characterized by warmer subsiding air mixing with cooler rising air, resulting in a subsidence inversion, identified by a negative gradient between the atmospheric and adiabatic lapse rate, or analogously, an increase in potential temperature (Jacob, 1999). At this height, sharp gradients in other atmospheric parameters such as aerosol concentration and water vapor density are also observed (Stull, 1988). The PBL reaches a maximum during mid-afternoon, when vertical mixing takes less than an hour (Jacob, 1999); hence, the distribution of air within the PBL is considered to be homogenous in contrast to the free troposphere. Subsequently, the boundary layer decays due to a decrease in sensible heat flux. In the early evening, the surface heat flux becomes negative, creating a stable boundary layer where turbulence is suppressed. Temperature inversions near the surface inhibit turbulence at night, prompting air mass stratification, and a lower boundary layer height than during the day (Nadeau et al., 2011). As a consequence, air quality may be compromised during the night, due to continuous pollutant emissions and transformations within a stable near-

surface regime (Salmond et al., 2005). Such night-time inversions are most common in the winter (Wallace et al., 2009). Mixing height also exhibits a seasonal dependency: the PBL reaches a maximum in the summer and minimum during winter (Cheng et al., 1997). Overall, mixing within the PBL takes 1 to 2 days, while surface emissions will reach the free troposphere (5 km) over the course of a week (Jacob, 1999).

2.12. Objectives

This study was designed to achieve the following objectives:

1) Ground level monitoring of NO_2 concentrations in different regions of Pakistan.
2) Comparison of NO_2 concentrations obtained with MAX-DOAS with results of satellite observations and in-situ measurements

Chapter 3

3. INSTRUMENTION AND METHODOLOGY

3.1. HAZ-Scanner (HIM-6000)

The portable HAZ-Scanner model HIM-6000 is an ambient air quality monitoring station capable of measuring several EPA-criteria pollutants and atmospheric variables. It can carry out simultaneous monitoring of $PM_{2.5}$, PM_{10}, and up-to 14 critical air parameters. In this research two HAZ-scanners were employed and placed in two different locations the specifications of these two instruments are mentioned in table 3.1.

Table 3.1: Instrument specifications for Haz-scanners used in this study

Specifications			Lahore Instrument	Multan Instrument
Sensor	**Technology**	**Range**		
$PM_{2.5}$	Gravimetric $PM_{2.5}$ impactor	2.5 µm	✓	✓
PM_{10}	Gravimetric PM_{10} impactor	10 µm	✓	×
Carbon Dioxide CO_2	NDIR	0 to 5000 ppm	×	✓
Carbon Monoxide CO	Electrochemical	0 to 10 ppm	✓	✓
Nitric Oxide NO	Electrochemical	0 to 5000 ppb	✓	✓
Nitric Dioxide NO_2	Electrochemical	0 to 5000 ppb (0 to 5 ppm)	✓	✓
Ozone O_3	Metal Oxide Semiconductor	0 to 150 ppb (0 to 0.15 ppm) or 0 to 500 ppb (0 to 0.5 ppm)	✓	✓
Sulphur Dioxide SO_2	Electrochemical	0 to 5000 ppb (10 to 500 ppb for ambient applications)	✓	✓

3.2. Mini Max-DOAS Instrument:

The mini-MAXDOAS instrument is a light weighted box with dimensions of 13cm×19cm×14cm. The instrument used in this study consisted of a 40mm front mounted lens, a Czerny-Turner spectrometer (USB 2000+, Ocean Optics In.), with a spectral resolution of 0.7nm, an installed stepper motor (with frequency of 444 for ISB-instrument, and 666 for field campaigns instrument) used to move the instrument to the desired elevation angle. The spectral range of the MAXDOAS instruments used in this study ranged from 320-460nm (ISB-Study site) and 314-445nm (LHR & MUL site). Scattered light was measured by the instrument through the lens (sealed to prevent the condensation of water vapors and intrusion of dust particles, which could damage the sensitive interior optics).

The passive DOAS measurements are based on the narrow-band absorption of sunlight by atmospheric trace gases, at known wavelengths in the UV/visible range. By comparing the intensity of sunlight within a required wavelength range, simultaneous daytime measurements of trace gases can be isolated from a series of continuously recorded spectra. The desire to gather information about trace gas behaviors with respect to mixing ratios, combined with a deeper understanding of radiative transfer modeling, prompted the development of off-axis DOAS, and subsequently, multi-axis DOAS (MAX-DOAS) (Kaiser, 1997; Hönninger and Platt, 2002; Wittrock et al., 2004). The MAX-DOAS instrument can be used to measure multiple trace gases in the visible and Ultra-Violet Spectral ranges and because of its low residuals it can be used even in less polluted environment.

Working Principle:

The sensitivity of MAX-DOAS measurements to trace gas absorption in the atmosphere at varying altitudes is dependent upon the location of photons scattered into the instruments line of sight. Vertical profiles of various trace gases can be inferred from the information obtained by

collecting spectra's at different elevations and using knowledge of photon trajectories and boundary layer dynamics.

Figure 3.1 highlights the sequence of ground-based MAX-DOAS measurements. The panel A show measurements at an elevation angle θ, having enhanced sensitivity to the presence of trace gases in the Planetary Boundary Layer. Panel B on the other hand shows zenith measurements largely representative of stratospheric absorption.

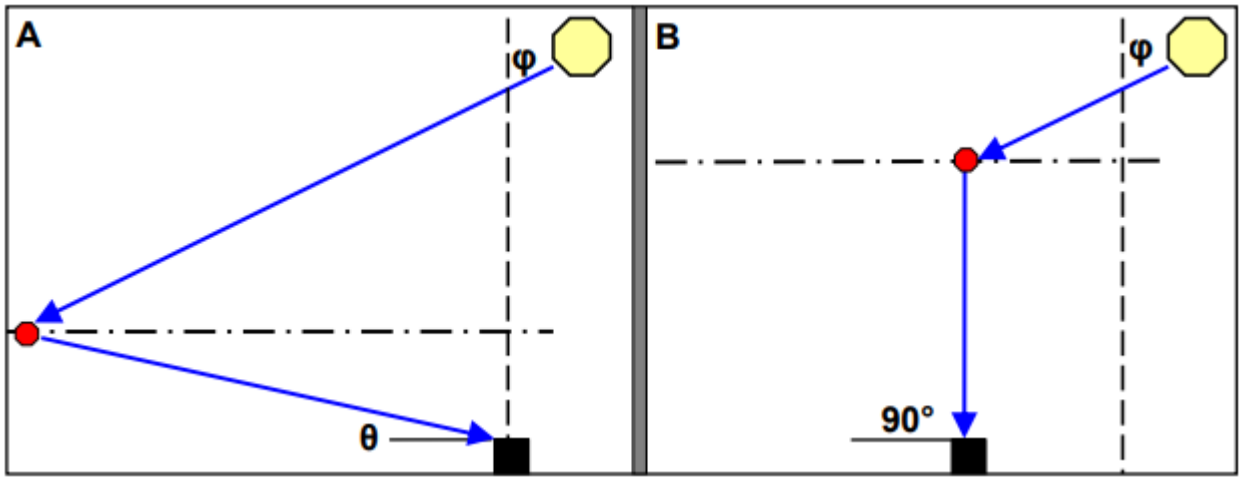

Figure 3. 1: Schematic for ground-based MAX-DOAS measurements at a designated relative azimuth angle (δ). Panel A highlights measurements at an elevation angle θ. Whereas, Panel B shows a measurement conducted under zenith geometry

The red circle in each panel of figure 3.1. represents a photon scattering event. In a Rayleigh atmosphere (i.e. an atmosphere that accounts for scattering only in trace gases and excludes the impact of aerosols and water vapors), measurements at lower elevation angles are more likely to observe scattering in the PBL (~ 500 m above ground level). Whereas, zenith measurements are predominantly subject to photon scattering in the upper troposphere (~ 9 km above ground level) (Hönninger et al., 2004).

Each spectrum recorded by MAX-DOAS is analyzed using the Beer-Lambert Law, which is modified to account for atmospheric narrow- and broad-band absorbance structures as follows:

$$In\ \frac{I_{90}\ (\lambda, L)}{I_{\theta}} = P(\lambda, L) + R(\lambda, L) + \sigma_i \Delta SCD_i$$

In the case of passive DOAS measurements, the total intensity of light refers to the spectral signature of the sun in the absence of atmospheric absorption, approximated using a spectrum recorded at an elevation angle of 90°(I_{90}°) within the same measurement sequence of off-axis observations as highlighted in figure 3.1. Because of this passive MAX-DOAS configuration, one can only extract trace gas information that is ―differential to I_{90}° (differential in this case refers to the principal part of change in a function with respect to the independent variable). Since the DOAS technique outputs a differential quantity, radiometric calibration of the instrument is not necessary (Hönninger et al., 2004). And the use of I_{90}° (also known as the Fraunhofer Reference Spectrum) within the same measurement sequence of off-axis observations removes most of the influence of stratospheric absorption from MAX-DOAS measurements.

The Beer-Lambert law highlighted in equation 7 below, highlighted the linear relationship between the transmittance of light and the concentration of a substance present in the optical path. Such that:

$$I(\lambda)=Io\ (\lambda)\ e - \alpha LC \qquad \text{Eq. 7}$$

Where, "Io" represents the incident intensity of incoming electromagnetic radiation and "I" refers to measured intensity. This technique depends upon the difference in wavelengths between the observed and reference spectrums. But because of similar absorption ranges, various trace gases can be all together obtained within a selected fitting interval. Therefore, specific cross sections of the desired gas must be taken into consideration when retrieving the differential slant column densities (dSCDs). DOAS technique are especially useful for the retrieval of trace gases with relatively short lifetimes in atmosphere like that of NO_2 and studying their vertical and diurnal profiles.

3.3. Tools utilized in this Research Work:

The successful retrieval, analysis and comparison of Nitrogen dioxide VCDs, point concentrations and satellite concentrations as well as retrieval and comparison of other variables were carried out using the various tools and algorithms mentioned in Table 3.2:

Table 3.2: Software used in this study

Sr. No.	Software	Purpose
1	Differential Optical Absorption Spectroscopy Intelligent System (DOASIS)	The OS for Max-DOAS used for measuring back-scattering and recording spectra's
2	Windows Differential Optical Absorption Spectroscopy (WinDOAS)	Used for the Convolution and Calibration of the MAXDOAS instrument through recorded spectra
3	QDOAS	Analysis of the measured UV-visible Spectras using specified fitting intervals and cross-sections to retrieve dSCDs
4	Microsoft Excel (v 2013)	For calculation of geometric AMF, and conversion of SCDs to VCDs, for various statistical analysis of data.
5	ArcGIS (v 10.3.1)	Interpolation of satellite data, representation and comparison of field campaigns, generation of maps
6	Haz scanner (v7_7_7)	For the retrieval of HAZ-scanner measurements
7	Google Earth Engine	For retrieval of satellite information, such as NO_2 timeseries from TROPOMI
8	Giovanni (NASA Portal)	For retrieval of satellite information, such as timeseries of OMI NO_2 measurements
9	SPYDER (Python 3.7)	For retrieval of Boundary Layer Height information from ERA-5 and conversion of NCDF to Excel timeseries

3.3.1. Differential Optical Absorption Spectroscopy Intelligent System (DOASIS)

DOASIS is the software package used to run the MAX-DOAS instrument, acquire spectra's, change elevation angles, control Peltier temperature and adjust the integration time for each spectra. DOASIS functions are based on commands run through it using a JavaScript script. Its functions include the calculation of a ring spectrum, which is essential for the analysis of

spectra's in QDOAS. Dark current and Offsets which are values used for the calibration and reducing errors in measurements. Dark current refers to a small current produced by photosensitive devices like spectrometer and its measurements require large exposure over very little integration time.

Dark current is small current that is monitored for photosensitive devices like spectrometer. For its measurement, large Tini (Exposure/integration time) and less number of scans are selected. Offset is the measurements recorded in "No photons" condition, in other words, it is measured in dark conditions. However, a smaller integration time and high scans are used for measuring offset spectra as shown in Table 3.3.

Table 3.3: Values used for Dark current and Offset measurements.

	Integration/Exposure time(milliseconds)	**Scan numbers**
Dark Current	3	10000
Offset	10000-20000	1

3.3.2. Windows Differential Optical Absorption Spectroscopy (WinDOAS)

3.3.2.1. Wavelength Calibration:

For wavelength calibration, WinDOAS (Windows Differential optical absorption spectroscopy) was used. Spectrum taken at noon was used for the calibration purpose (usually taken at 90^{o} of noon time/with least SZA). In calibration, the fit was applied between a measured and a convoluted spectrum. Meanwhile, wavelength of the solar spectrum was attributed to the individual detector's pixels (2048). The calibration fit is also known as "Kurucz-fit" because a solar spectrum measured by Kurucz is usually used as input which is further convoluted as per the spatial resolution of the mini-MAX-DOAS used in the monitoring. The wavelength range was divided into several sub-windows (subwindows= 6) for analyzing the fits in each sub-window. For adjustment of spectrum shift between convoluted

and measured spectra, "shift and squeeze" was also applied. Slit Function Parameter (SFP) specifies that the interpolation of the results of the individual sub-window were carried out using polynomial degree. Repeated twice the calibration process, reduces the residual. All measure spectra are evaluated in this study using the calibration file against a reference spectrum.

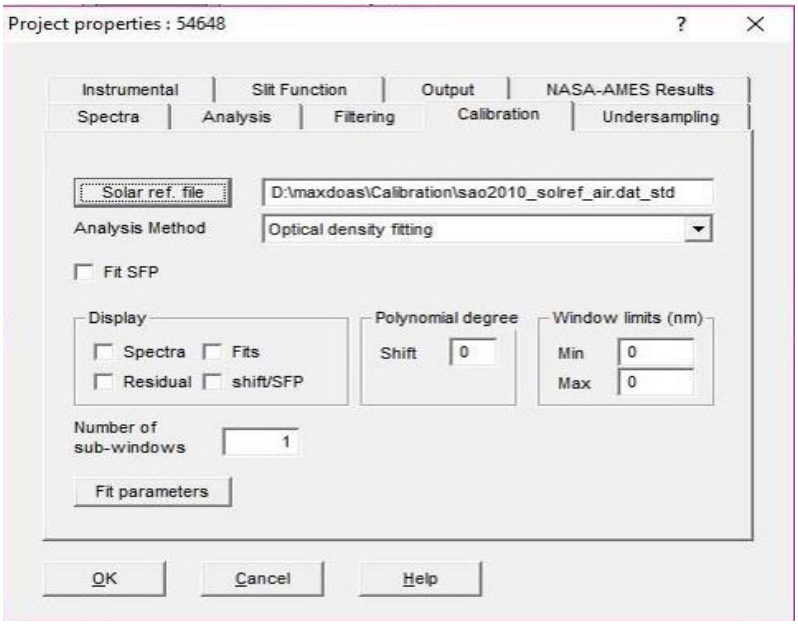

Figure 3. 2: Calibration window for WINDOAS

3.3.2.2. Wavelength Convolution:

This process was performed by using "Convolution tool" of WinDOAS software. It is a mathematical process which is important for wavelength processing operations.

3.3.2.3. NO_2 Analysis:

This is performed in QDOAS software. Selected NO_2 analysis window was 409 nm to 445 nm. The wavelength range was chosen because of lowest possible residual errors and DOAS fit result. For analysis, calibrated spectrum was used as reference spectrum. Different crosssections: NO_2 at 298K (Vandaele et al., 1996), NO_2a at 220K (Vandaele et al., 1996), O_3 at 223K (Serdyuchenko, Gorshelev, Weber, Chehade, & Burrows, 2014), O_4 at 293K (Thalman & Volkamer, 2013), H_2O (Rothman & Transfer, 2010) and Ring were used. Polynomial of 4th

degree was used for NO_2 analysis. Some fields/parameters in the "Output Tab" were selected which is required in the results i.e., Solar zenith Angle (SZA), RMS (root mean square/residue), Elevation viewing angle and integration time etc. Then finally, the output file path was given where the files wanted to be stored. The analysis was performed on all measured spectra and NO_2 dSCDs and results were obtained in ASCII file.

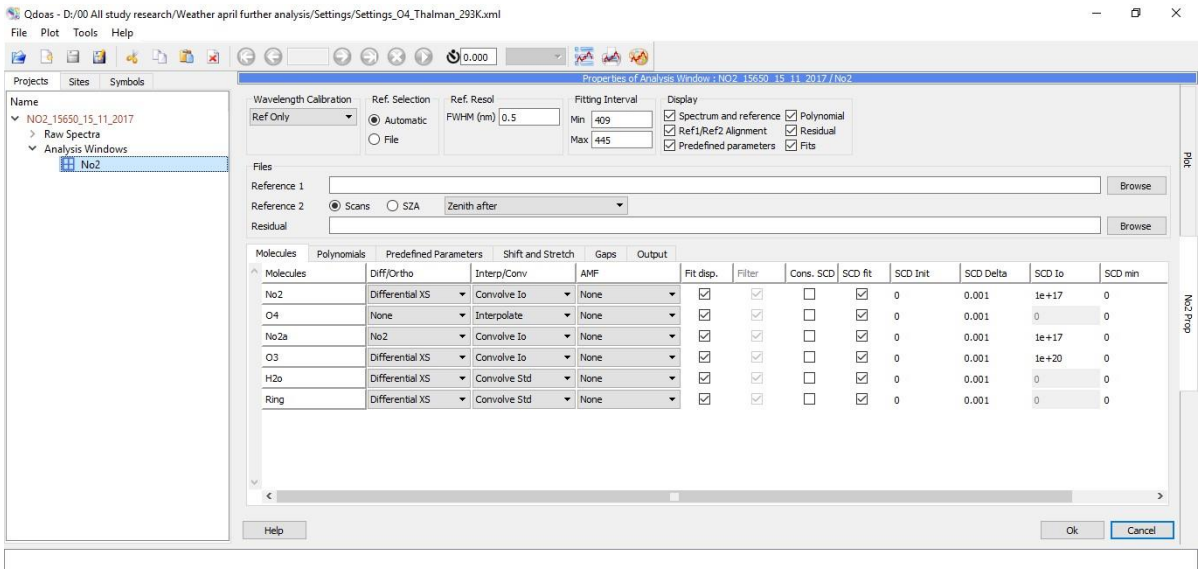

Figure 3. 3: NO2 Analysis window in QDOAS, showing fitting interval used for Nitrogen Dioxide

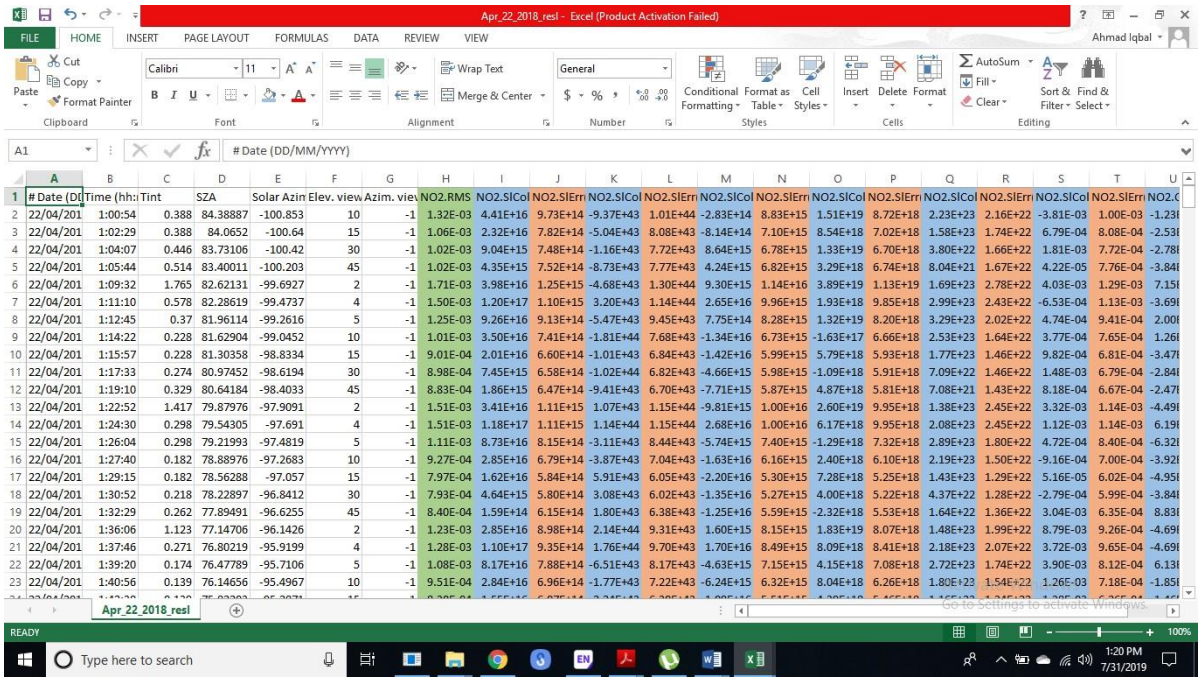

Figure 3. 4: ASCII files obtained by QDOAS; green column representing RMS, blue columns showing dSCDs, brown columns illustrate slant column errors

Figure 3.5 shows example of DOAS fit for NO_2. Red lines represents the reference spectrum and black line shows the measured spectrum after subtracting all other absorbers. It was measured on 23 May 2018 at 12:36 UTC. SZA was 73° and elevation angle was 5°. Mean dSCD value for this fit was 3.55×10^{16} molecules cm^2.

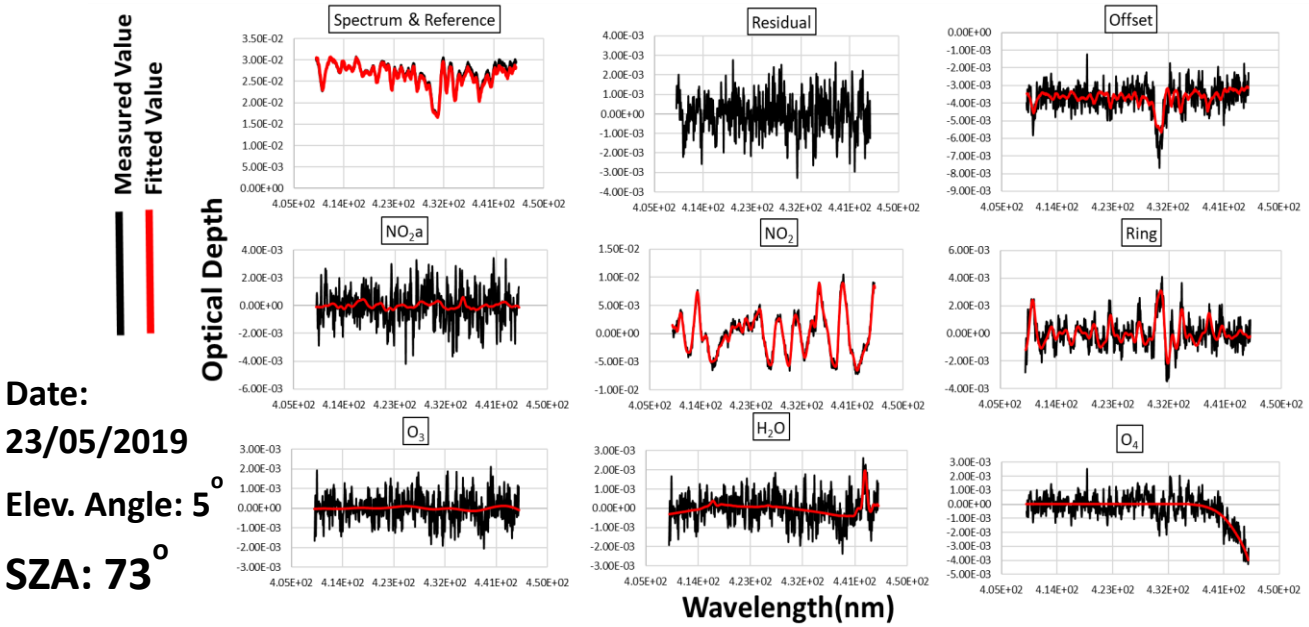

Figure 3. 5: Nitrogen Dioxide DOAS fit measured on 23 May 2019 at 12:36 PST

3.4. Air Mass Factor and NO_2 VCD Extraction Calculation using MS Excel

Microsoft Excel was used in this study to calculate NO_2 VCDs by using geometric air mass factor application. AMF is ratio of actual path distance of solar radiations and vertical path. AMF calculations are used to convert the SCDs (Slant column densities) into VCDs (Vertical column densities). Air mass factor (AMF) is usually calculated using radiative transfer model but in this study, AMF was estimated using geometric approximation method (Hönninger et al., 2004; Wagner, Ibrahim, Shaiganfar, & Platt, 2010). This method allows the retrieval of column densities of trace gases even in cloudy conditions (Wagner et al., 2010).

$$VCD = SCD/AMF \quad \text{Eq. 9}$$

Here differential air mass factor (dAMF) is used because the slant column densities obtained were differential SCDs (Liu et al., 2016):

$$VCDtrop = dSCD\alpha / dAMF\alpha \quad \text{Eq. 10}$$

dAMF is difference in AMF obtained at a certain angle and AMF obtained at 90^o:

$$dAMF\alpha = AMF\alpha - AMF_{90^\circ} \quad \text{Eq. 11}$$

So, eq (10) will be:

$$VCD_{trop} = dSCD\alpha / AMF\alpha - AMF_{90^\circ} \quad \text{Eq. 12}$$

Using geometric approximation, AMF can be found as:

$$AMF = 1/\sin\alpha \quad \text{Eq. 13}$$

Then Eq. (12) will be:

$$VCD_{trop} = dSCD\alpha / 1/\sin(\alpha - 1) \quad \text{Eq. 14}$$

4.RESULTS AND DISCUSSION: Chapter 4

4.1. Results from IESE-site Islamabad

4.1.1. MAX-DOAS observations

Daily MAXDOAS observations from September 2015 to September 2019 taken between 1-2 pm PST and compared against OMI (Ozone monitoring instrument-present on to the Aura-satellite) and TROPOMI (TROPOspheric Monitoring Instrument present on the Sentinel-5P satellite).

The comparison of daily observations available for all three instruments is presented in Fig. 4.1 The data for ground-based MAX-DOAS and OMI-satellite observations, excluding January and February 2016 was available from September 2015 to September 2019. The data for TROPOMI was available from September 2018 onwards. According to figure 4.1, MAXDOAS and both OMI and TROPOMI show similar trends during the entire study period. However, satellite observations significantly underestimate the observations as compared to ground-observations. This is most likely a result of the low sensitivity of satellite observations to changes in Boundary dynamics. Among satellite observations TROPOMI observations are consistently higher than OMI observations, a major reason for this might be because of the difference in resolution between the two instruments. TROPOMI has a resolution of around (7 × 3.5 km) as compared to OMI, which has a lower spatial resolution of 13 × 24 km.

From figure 4.1.(a) we can see seasonal variation in the daily NO2 measurements, which are minimum during summer months and maximum during the winter months. Most likely because of the meteorological conditions, such as lower boundary layer heights in winter periods which can lead to restricted movement of atmospheric pollutants. The monthly average concentrations shown in figure 4.1(b) we can see the same trend carries out across the year, with higher concentrations in winter followed by lower concentrations during summer and monsoon months.

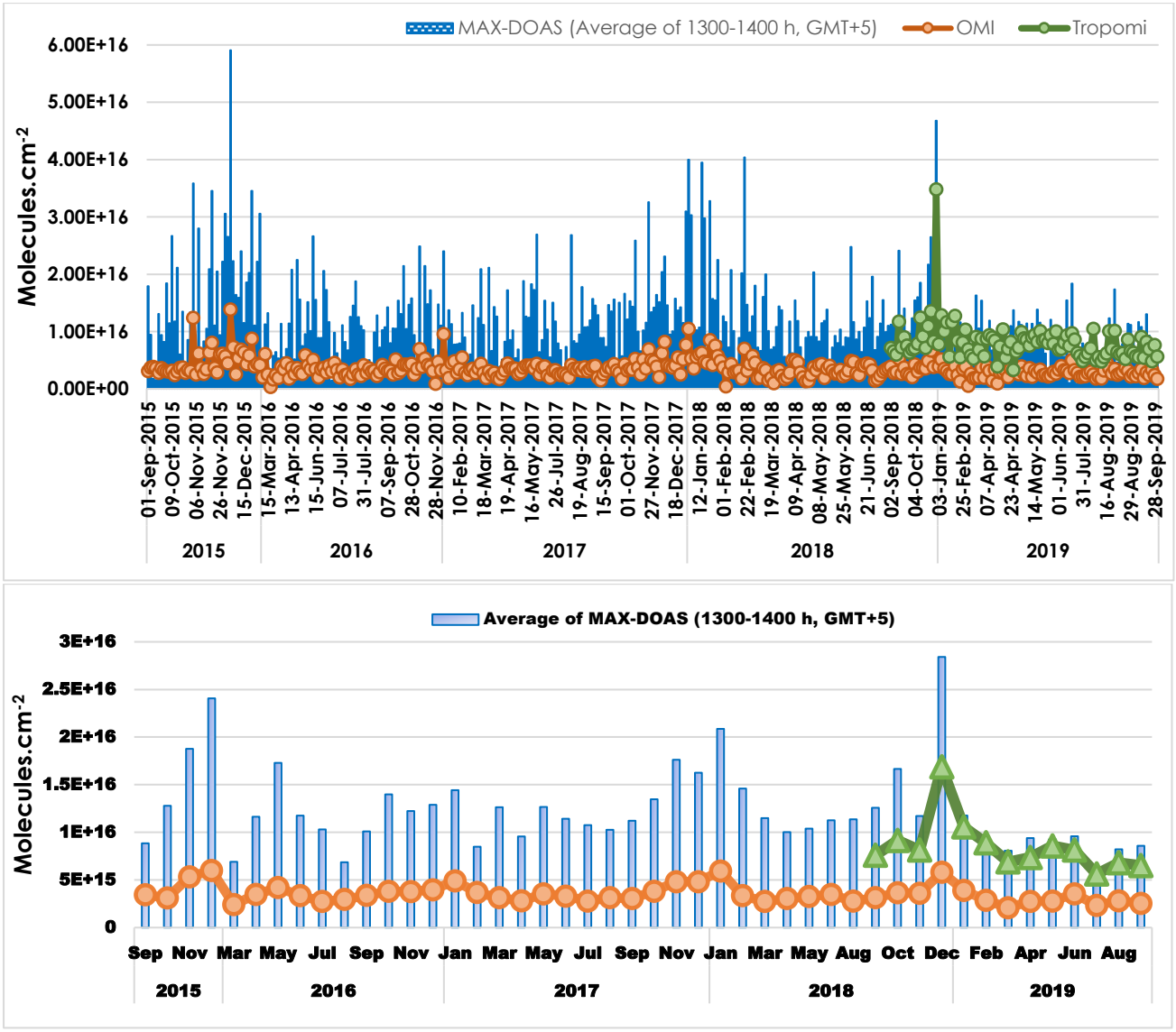

Figure 4. 1: Comparison of daily vertical column densities (VCDs) in molecules cm-2 retrieved through ground-based MAX-DOAS, OMI & TROPOMI from 2015-2019. (b) Comparison of average monthly vertical column densities (VCDs) in molecules cm-2 retrieved through ground based MAXDOAS

Figure 4.2 highlights the comparisons made between all three instruments and according to these comparisons MAXDOAS and TROPOMI observations show the highest correlation for both daily and Monthly observations. A major reason for this could be the difference in resolution and monitoring capabilities, TROPOMI observations have been reported to far more accurate as compared to OMI and its predecessors (SCIAMACHY, GOME & GOME-2).

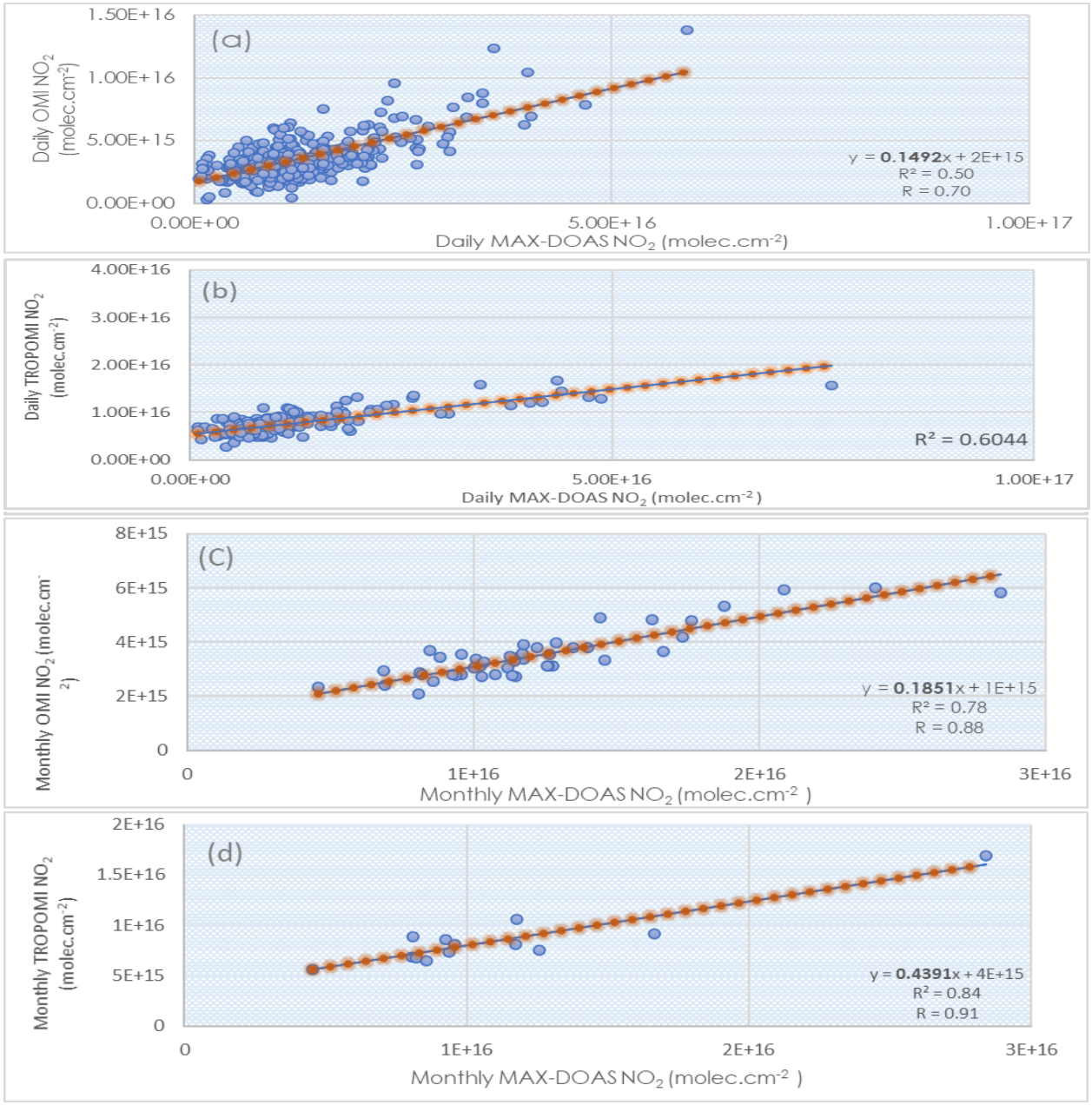

Figure 4. 2: (a) &(b) Comparison of Daily MAXDOAS observations obtained using MAXDOAS, OMI & TROPOMI.

Another possible reason for the difference in comparisons could be the difference in number of quantities compared, with OMI observations being available for a far longer time, it is likely that more variations may have compounded over this longer period.

Figure 4.3. Shows the diurnal variation in daily MAXDOAS observations, according to this graph. Daily NO_2 observations are minimum during periods of low-light such as early mornings and reach lower concentrations as sun-light induced photolysis occurs. Between 10 am to 12 am

the sun-light induced photolysis leads to lower concentrations of NO_2 in the atmosphere. However, these low concentrations are soon offset by vehicular traffic emissions which lead to higher NO_2 concentrations. Soon afterwards higher concentrations of NO_2 are built-up in the atmosphere and remain their until the next day.

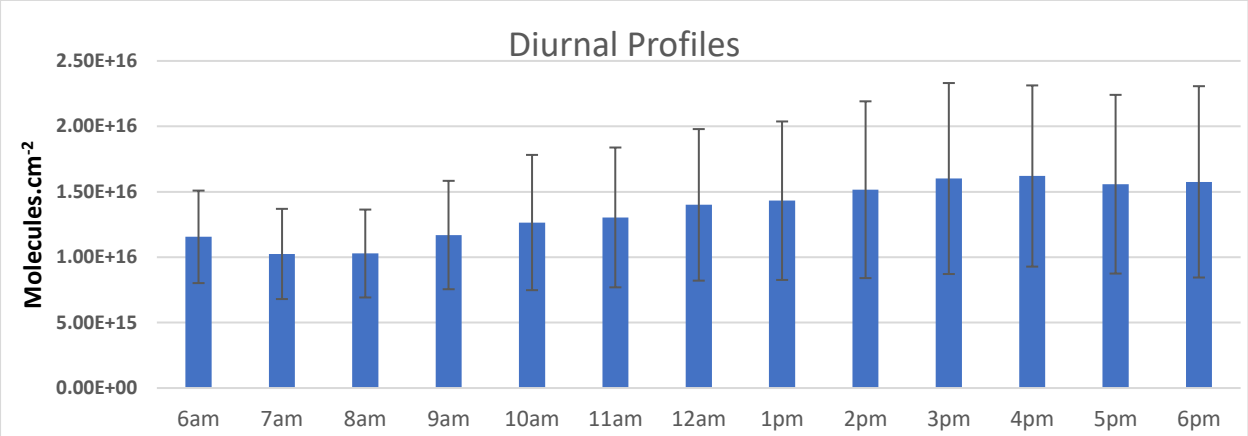

Figure 4. 3: Diurnal variations in daily MAXDOAS Observations.

4.1.2. Satellite observations

Figure 4.4. Shows the seasonal variation in daily satellite observations obtained from TROPOMI (from 2018-2020), according to this graph. Daily NO_2 observations are minimum during the months of pre-monsoon, monsoon periods are also relatively low with some sporadic rises and falls in concentrations. Winter periods show highest concentrations followed by post-monsoon periods most likely because of stable boundary layer dynamics.

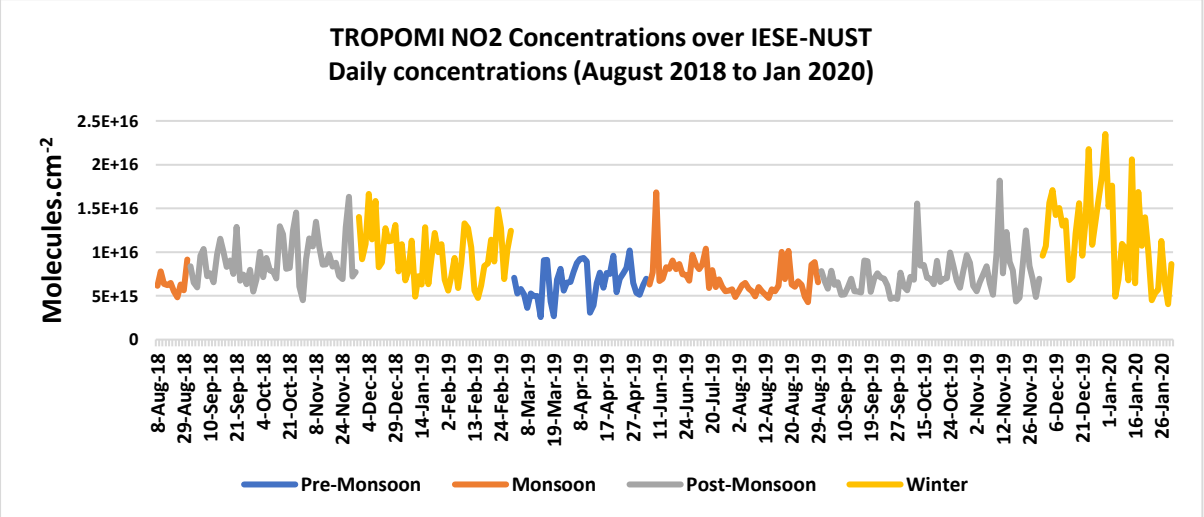

Figure 4. 4: Seasonal trends in TROPOMI NO2 observations observed over IESE 2018-2020

Figure 4.5 shows the monthly averaged NO_2 tropospheric vertical column densities obtained using the OMI-instrument. The seasonal trend observed in figure 4.4. shows that throughout the year in Islamabad concentrations of NO_2 rise during the period of winter and fall during the period of monsoon. Most likely driven by stable boundary layer conditions in the winter and abundance of OH radicals in the monsoon periods.

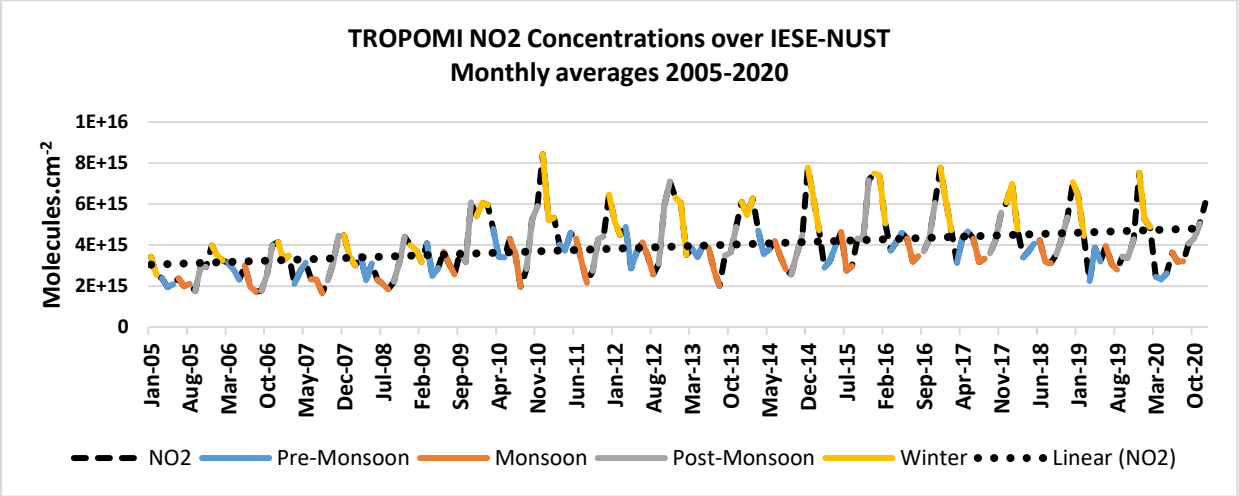

Figure 4. 5: Seasonal trends OMI NO2 observations observed over IESE 2005-2020

4.1.3. Comparison of Meteorological variables and MAXDOAS observations

Figure 4.6 highlights the comparison of daily MAXDOAS observations (6am-6pm) with Meteorological observations available from 2018-2020. According to this figure, MAXDOAS observations and NO_2 measurements correspond strongly with lowering boundary layer conditions, lower temperatures and low global horizontal irradiance. And high-temperatures, high boundary layer heights and strong GHI correspond with low NO_2 values.

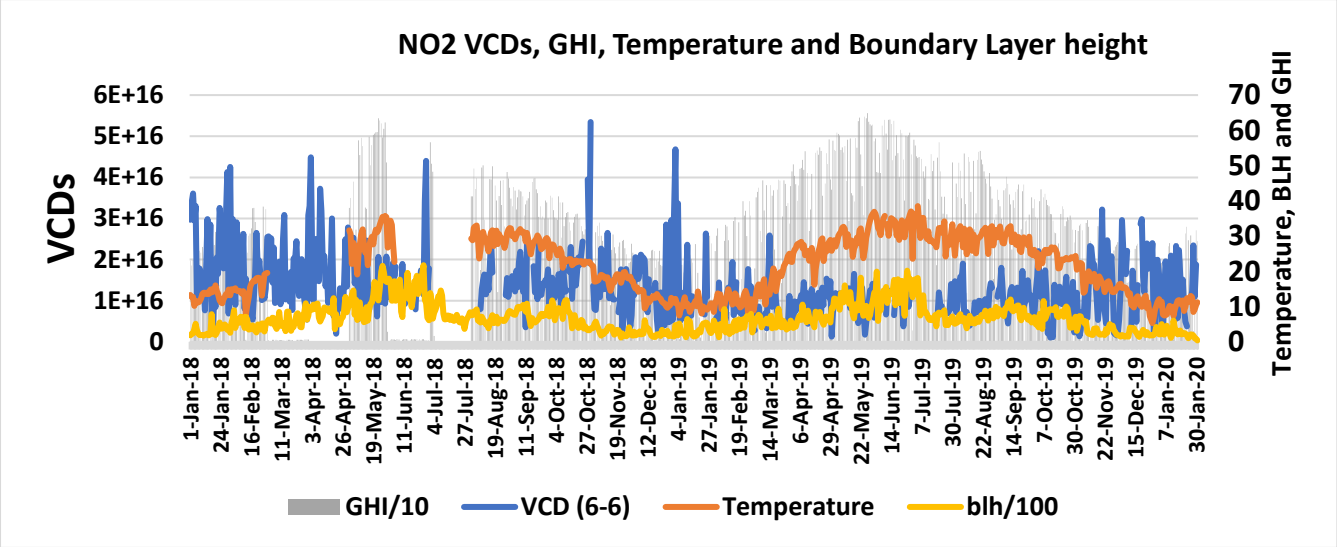

Figure 4. 6: Comparison of daily NO2 VCDs against Meteorological parameters over IESE-NUST 2018-2020.

According to the data recorded in this figure seasonal NO2 variations are strongly driven by meteorological conditions and thus monitoring meteorological shifts can help understand changes in pollutant concentrations and help build planning and preparedness in a population for poor air quality situations. When temperature and global horizontal irradiance is high, more photolysis activity is likely to take place leading to lower concentration of NO_2, whereas in lower boundary layer conditions the pollutants there is less convection and thus atmospheric cleaning capacity is reduced leading to build-up of pollutants.

4.2. Results for Lahore & Multan

4.2.1. Comparison of meteorological data

Climate and weather can influence air quality through many interrelated pathways. Therefore, it is necessary to explore the meteorological conditions for a better understanding of their linkage with air quality conditions of the selected study sites.

The definition of fog and smog is described in the following passage for a better understanding of the natural phenomenon and how it is impacted by anthropogenic activities. As per textbook definitions (Ahren and Henson 2015), the essential parameters for fog formation are listed as:

1. Visibility should be less than 1000 m

2. Availability of aerosols (AOD should be greater than 0.4 a proxy indicator)

3. Humidity should be greater than 75%
4. Dew point temperature difference (ambient - dew point temperature) should be less than or equal to 10 °F.

According to Pakistan Meteorological Department (PMD), fog is further characterized into the following categories based on visibility conditions (see Yasmin et al., 2012) as under:

- very Dense Fog: visibility < 50 meters
- Dense Fog: visibility < 200 meters
- Moderate Fog: visibility < 500 meters
- Shallow Fog: visibility < 1000 meters
- Haze and Mist: visibility > 1000 meters

Visibility data for the months of winter (Oct. to Feb.) from the years 2015 to 2020 is presented in this section for both study sites of Multan and Lahore. The bar charts in Figures 4.7 & 4.8 highlight the %age of visibility incidences i.e. the occurrence of haze, shallow fog, moderate fog, and dense fog incidents characterized based on visibility conditions. The discrimination between fog and haze incidents was made by following the PMD criterion described by Yasmeen et al., (2012).

Figures 4.7 shows the visibility data for Multan for the months of October, November, December, January, and February since 2015. The month of January shows the peak value of dense fog (usual winter fog) each year from 2015 to 2020 in Multan. The month of December witnessed high dense fog events for averages in the years 2016, 2017, and 2019. A very small value of fog may be seen in the December of the remaining years such as 2015 and 2018. The month of November observed high values of dense fog only in 2017 while February has high values both in 2018 and 2019.

Figure 4.8 shows the visibility data for Lahore. In Lahore, the month of December shows extremely high values of dense fog for the years 2016 and 2019 while minor values during the rest of the years. November has shown high numbers during 2017. The month of January displays a consecutive high value in 2017, 2018, and 2020, with a relatively visible large number in 2016 as well. October has also received its share of dense fog concentration in 2016 and 2017. Figure 4.8 shows dense fog events for all the observed months i.e. October, November, December, January, and February for the year 2017.

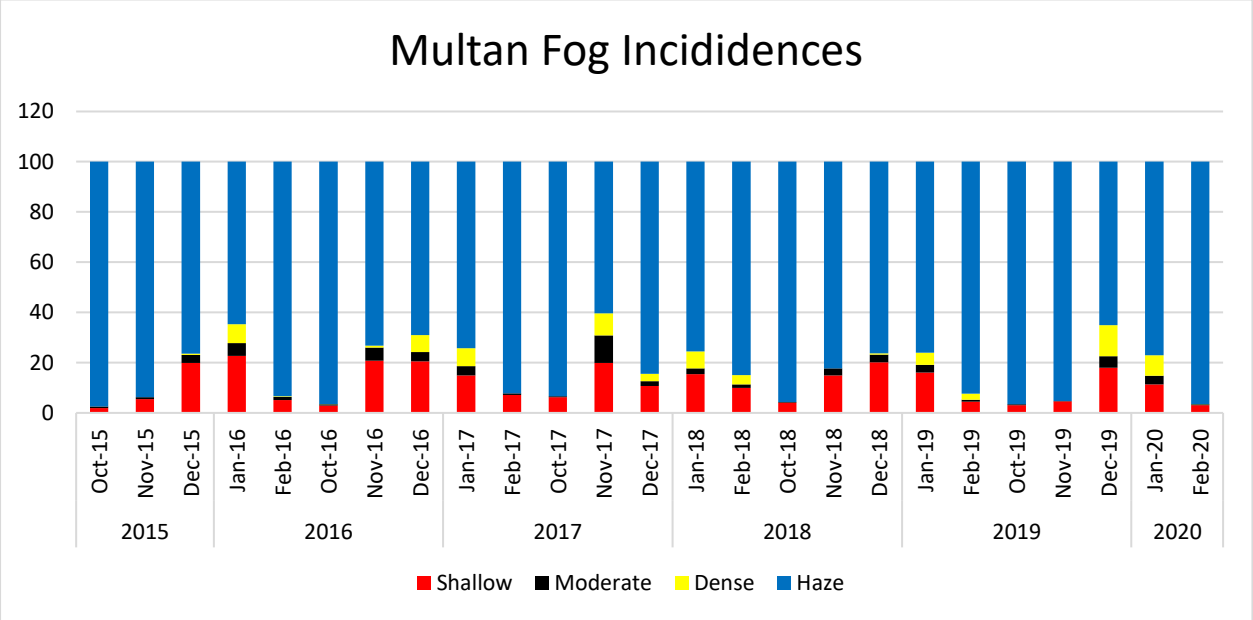

Figure 4. 7: Chart representing monthly averages of Haze, Shallow fog, Moderate fog, and dense fog over Multan for five years based on visibility conditions.

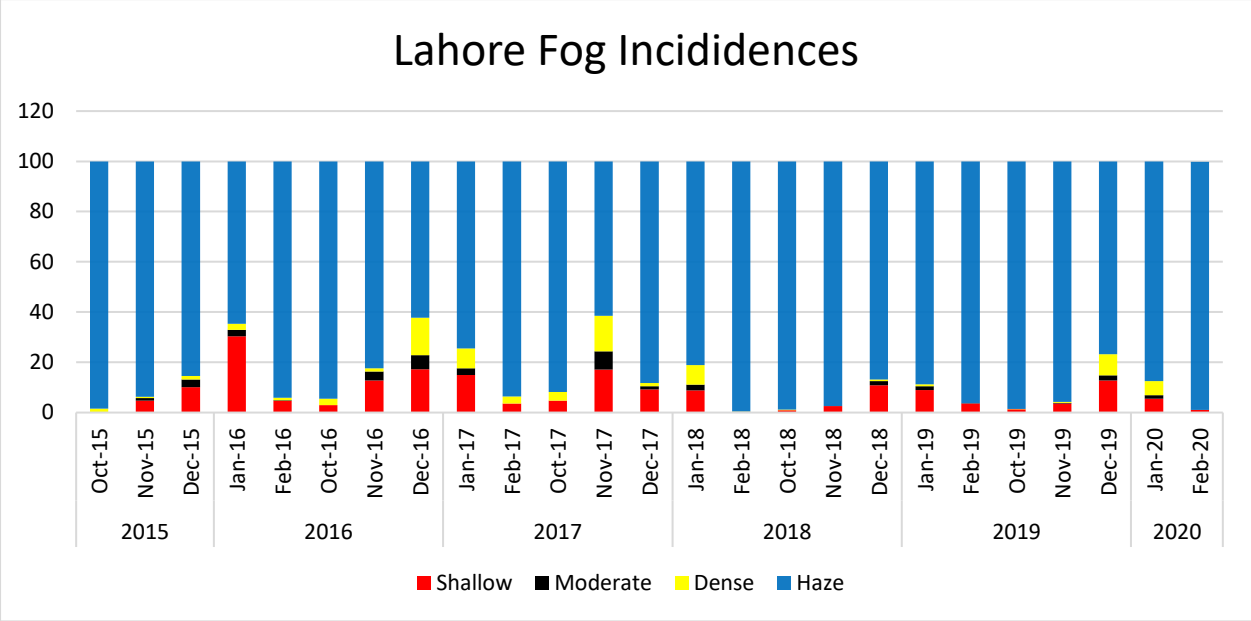

Figure 4. 8: Chart representing monthly averages of Haze, Shallow fog, Moderate fog, and dense fog over Lahore for five years based on visibility conditions.

There has been no consistent behaviour in the fog incidences observed during the selected period of 2015 to 2018. However, it has been consistently found that a higher number of dense, moderate, and shallow fog events are frequent during the months of December and January (winter fog) only. However, there have been more or less very few radiation fog incidences observed during the months of October and November which can be attributed to factors other than radiation fog events such as fire smoke.

The frequency of fog incidents escalates with a decrease in temperature and result in reduced visibility in the study area (e.g. Wu et al., 2017). Similarly, meteorological parameters i.e. temperature, atmospheric pressure, and humidity for the period of four months are shown in Figure 4.9 The purple lines in figures 4.9 represent the number of incidences based on low visibility i.e., visibility < 1000 m.

According to the prescribed criteria (Ahren and Henson 2015), visibility can be taken as a precursor/indicator for assessment of air quality but to term it as a radiation fog event one should be very careful, and all four criteria should be fulfilled. In Multan 4.9 (b), low visibility events correspond with incidences of high humidity, low temperature, wind speeds & (Boundary Layer

Height) BLH. This indicates that the yearly smog incidences recorded in Multan are a direct result of meteorological parameters and thus do not show any explicit seasonal trends. Although the visibility incidences are less in 2015, still the first minor peak is observed in the first week of November. The following year of year2016, high peaks are observed around 8th November. In 2017, the incidences started around the last days of October while reaching a peak in the first week of November. The peaks in 2018 are small yet seen around 31st October and 1st November. In 2019 the incidences have moved backward with observed peaks in mid-October and high peaks in the last week of October. The incidences have moved backward over the last five years from the first week of November to the last week of October.

In the case of Lahore 4.9 (a) during 2015 being the normal year, the reduced visibility started during the first week of November, however over the years, the number of reduced visibility incidence started moving towards the last week of October. While during the December months during all years, the majority of dense smog incidences occurred, which is further supported by meteorological conditions and reduced boundary layer height. There is one-week earlier initiation of the occurrence of reduced visibility incidences in the case of Lahore. However, the number of fog/smog incidences are inconsistent over the year as there is no exact pattern. A closer look into data for all 4 criteria, it can be concluded that during the month of October and November the reduced visibility is not due to radiation fog (the usual phenomenon in winter), as the humidity was quite low, with high temperature, wind speed, and relatively normal BLH condition. It can be attributed to the primarily smoke of rice paddy fires in India, which have hampered the visibility on either side of the border.

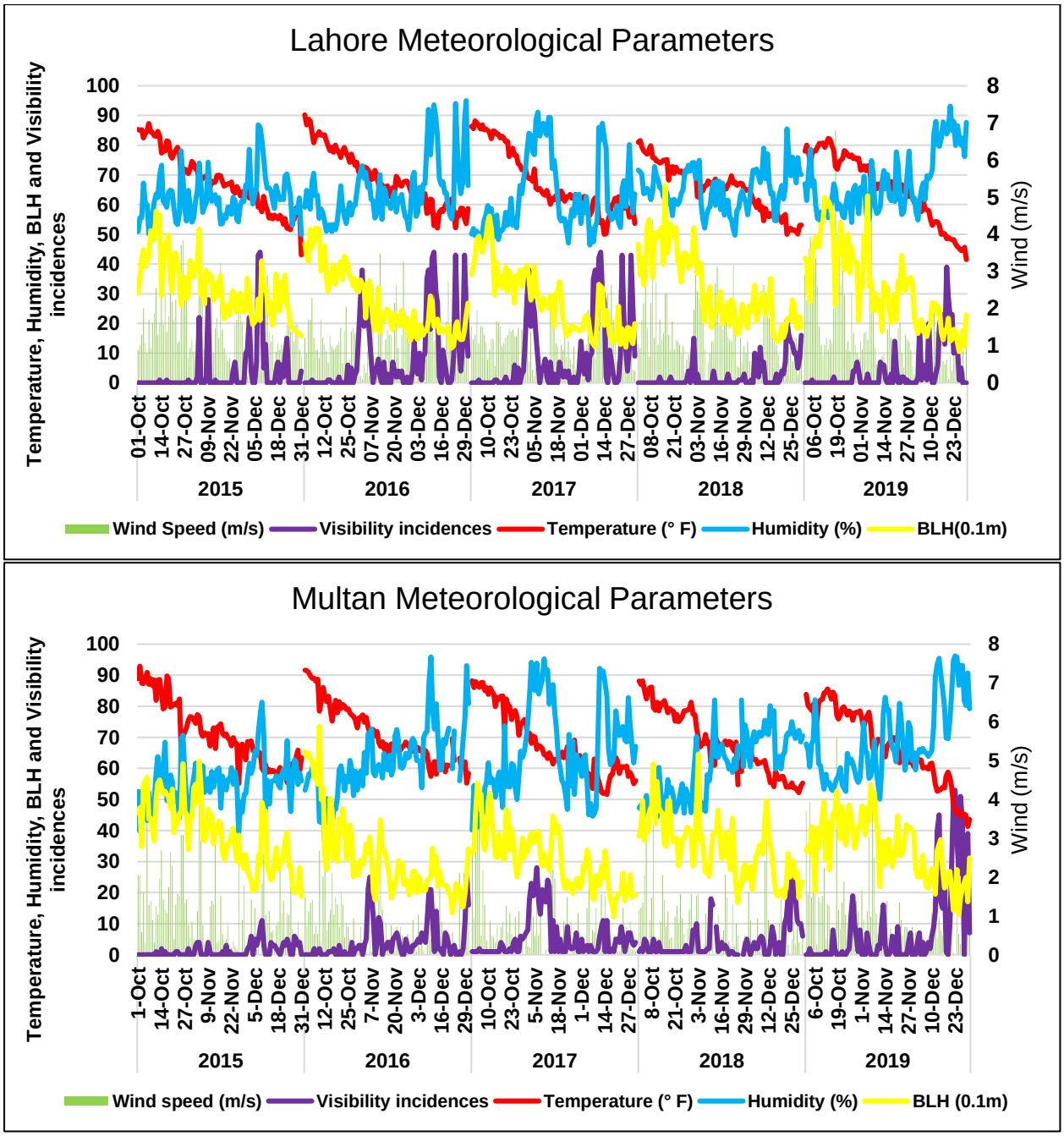

Figure 4.9: Comparison of Fire-activities, PM2.5 (Lahore and Delhi) and Delhi 5 years.

Therefore, the socio-economic disruptions in the Indian sub-continent around the first week of November (post-monsoon season) were caused by the massive smoke of rice paddy fires and consequently reduced visibility and deteriorated air quality conditions. However, there is consensus among the scientific community that low-visibility events irrespective of their origin/causes (fog/smog/smoke) can cause a huge economic burden to air and road transportation and highly damaging to human health (Fu et al., 2014).

4.3. Exploring the role of Agricultural fires in Air quality

Nitrogen dioxide through its various chemical pathways leads to the production of $PM_{2.5}$. A pollutant very important for health. Basic information on $PM_{2.5}$ has only recently become available for all South Asian countries including Pakistan through the AirNow Department of State program which has placed monitors at US Embassies and Consulates throughout South Asia.

Because of the similarity in the monitoring method and quality of data, it was used to demonstrate the spatial and temporal trends across two closely located South-Asian cities Lahore and Delhi. Data from the US Embassy in Delhi which goes back to January 2015 has been used to compensate for the lack of data in Lahore (available since May 2019. To demonstrate that this similarity in trend between the two cities is correct, Figure 4.10 offers both a recent comparison data for the two cities and retrospective data for Delhi showing the seasonal nature of the problem. MODIS fire counts included in Figure 4.10 (panel 3) are for the region between Lahore and Delhi which includes the Indian states of Punjab, Haryana and Uttar Pradesh and the Punjab province of Pakistan.

In both cities, $PM_{2.5}$ is at its lowest at the end of the monsoon season (Jul-Sep) before an abrupt increase occurs in mid-October. Long-term observations of $PM_{2.5}$ in Delhi from 2015-2019 along with MODIS active fire counts show this increase to be associated with agricultural burning, but the elevated $PM_{2.5}$ levels persist well beyond the burning period throughout the winter months. Thus, to fully understand the factors controlling air pollution for these two cities and the greater region, information must be gathered on sources that include more than just the seasonal agricultural burning that is concentrated in the northern Indian province of Punjab directly between these two cities.

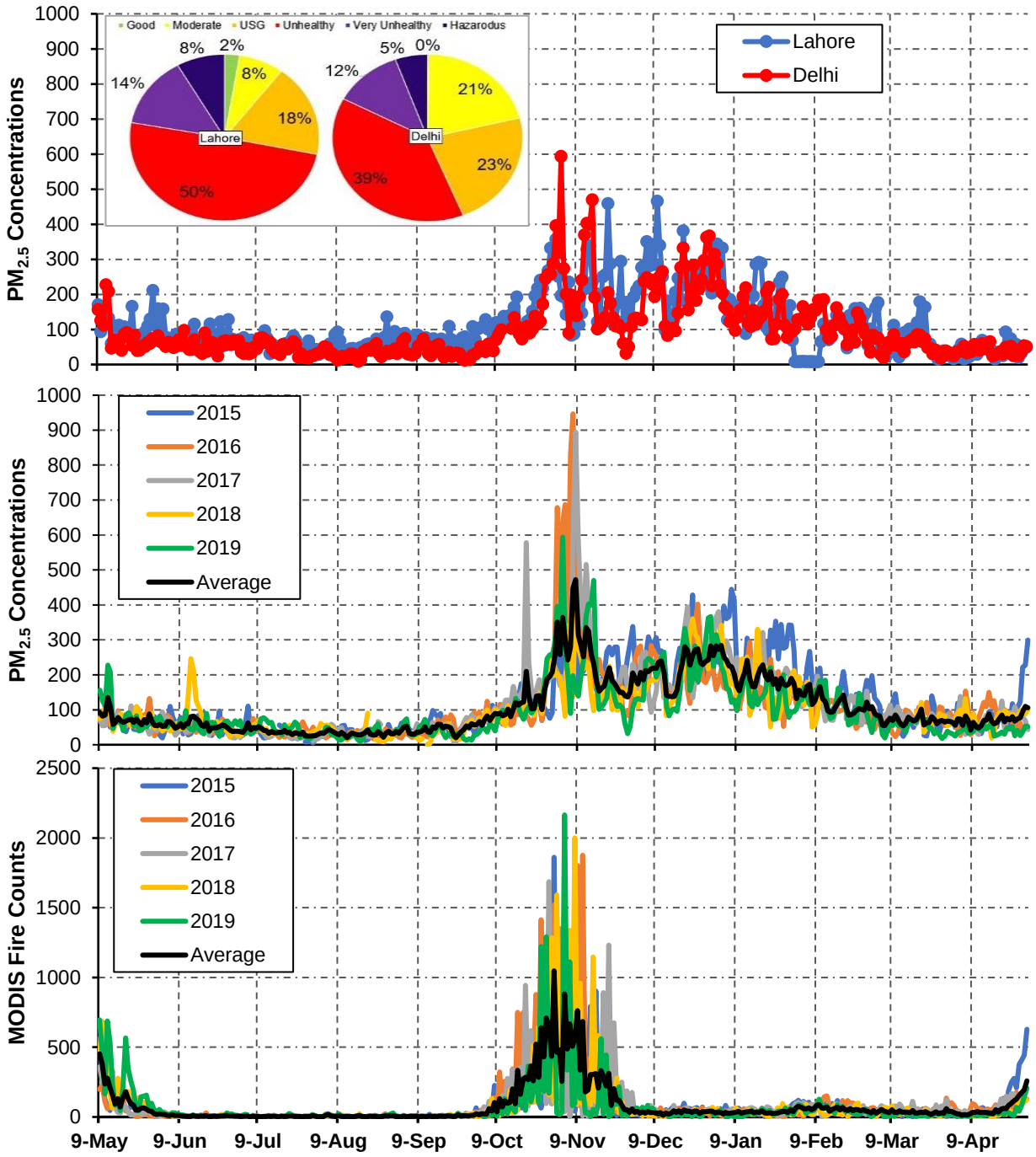

Figure 4.10: Comparison of Fire-activities, PM2.5 (Lahore and Delhi) and Delhi 5 years

4.4. Car MAX-DOAS observations in Lahore & Multan

Car based MAX-DOAS observations (where the MAXDOAS instrument was mounted on the roof of a car and driven across the city) were performed along the ring road (encircling most of the residential areas and industrial units) of Lahore. Additionally, wind data and satellite observations were obtained and used to interpret the results (represented below as wind vectors in each case and colored Tiles in the background with satellite coverage). Figure 4.11 shows the track for MAXDOAS field campaigns in Lahore along with locations for heavy traffic and industrial estates.

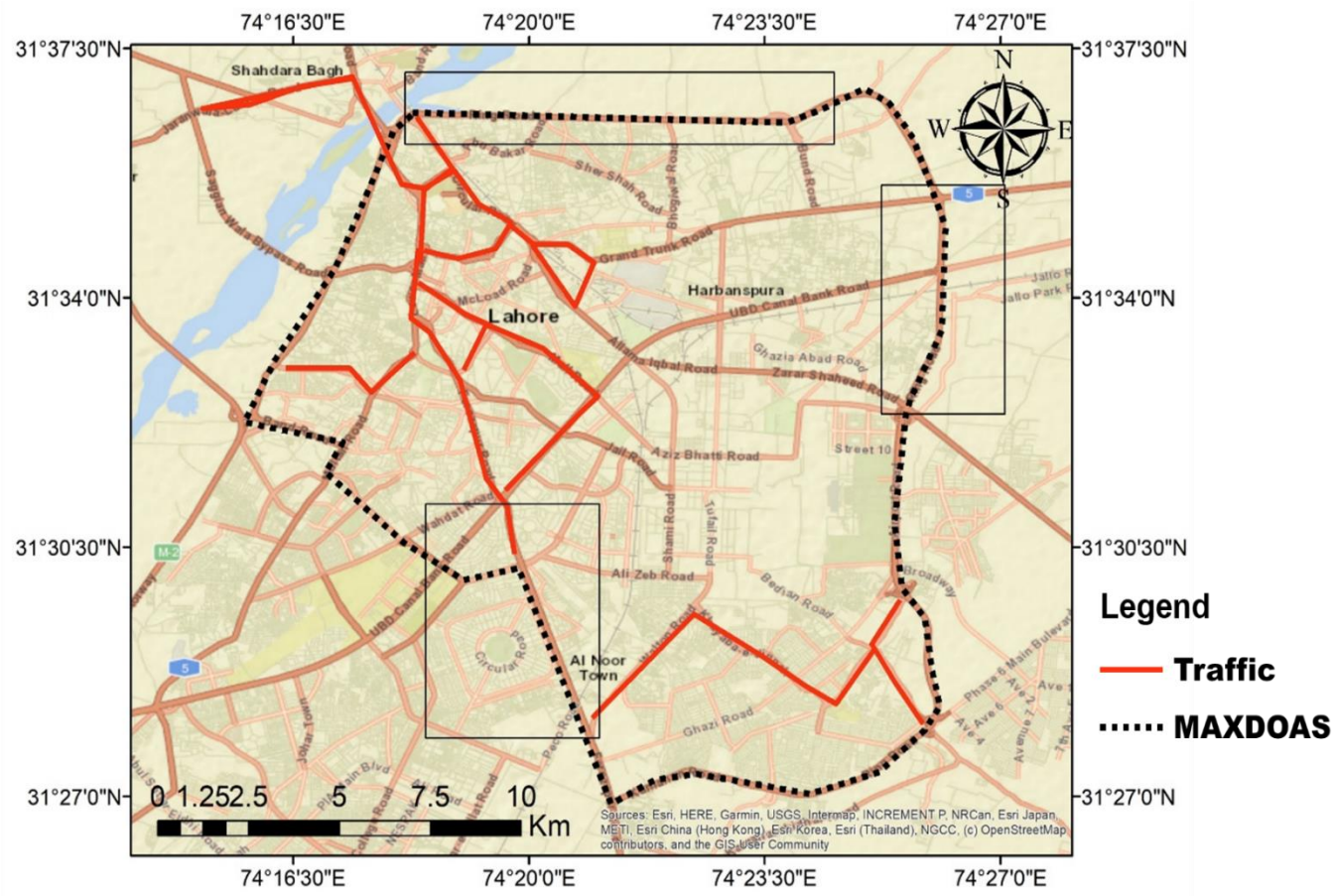

Figure 4. 11: Track for MAXDOAS field campaigns in Lahore.

Results presented in figure 4.12 show high columns of NO_2 around areas with heavy industry, dense traffic, or both. For instance, in Lahore, the highest columns of NO_2 were observed near Ravi Bridge during periods of heavy traffic and congestion episodes. Other parts of the ring road

also showed high levels of pollutants even during off-peak hours, such as the section from Bhatti Chowk to Lakhodair (which contained large quantities of steel and rubber industries, brick kilns, cold storage facilities, a 220kV grid station, and a large diesel engine workshop).

This section also contained the Mehmood Bhooti open dumpsite as well as the (Lahore Waste Management Company) LWMC compost plant a relatively high level of pollutants was observed in this section during many field campaigns.

Another section of the ring road from Lakhodair to Airport road also showed relatively high columns during most field campaigns, most high columns can be traced to the dense population surrounding this area and proximity to cottage industries.

The results from these field campaigns show higher columns of NO_2 around densely populated areas during school and office timings indicating that traffic is a major component in atmospheric NO_2 levels in Lahore. The wind data also shows a certain trend where in most cases the pollutant levels are higher in the direction of the downwind, especially when moving from industrial areas.

NO_2 Lahore 1st November 2019

Round 1 (Wind speed 3 km/h)

NO_2 Lahore 1st November 2019

Round 2 (Wind speed 3 km/h)

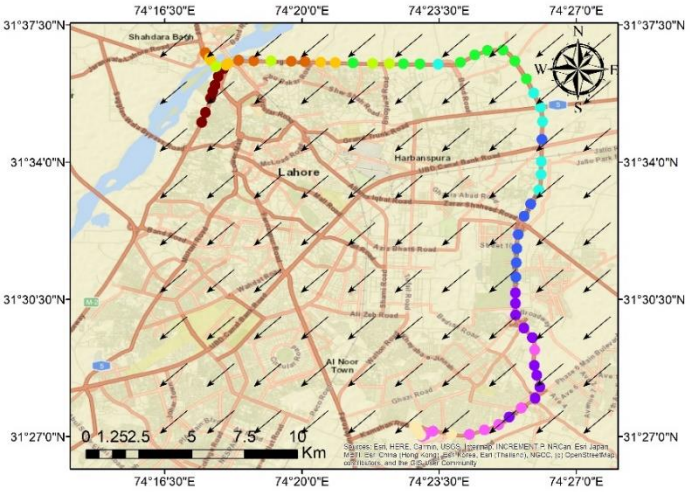

NO_2 Lahore 1st November 2019

Round 3 (Wind speed 8 Km/h)

NO_2 Lahore 2nd November 2019

Round 1 (Wind speed 7 Km/h)

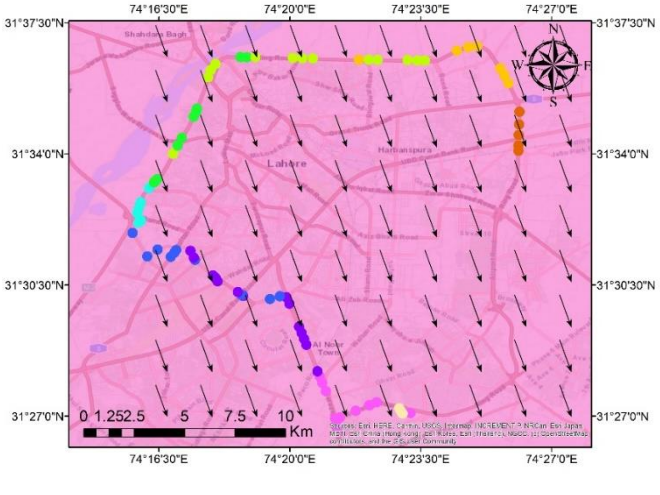

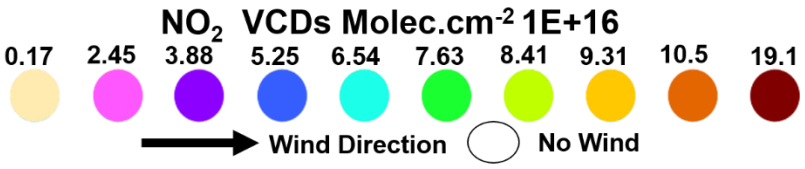

NO_2 Lahore 2nd November 2019

Round 2 (Wind speed 7 Km/h)

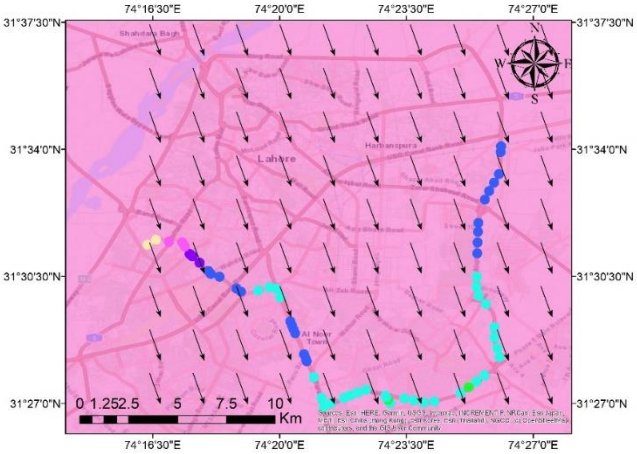

NO_2 Lahore 3rd November 2019

Round 1 (Wind speed 8 Km/h)

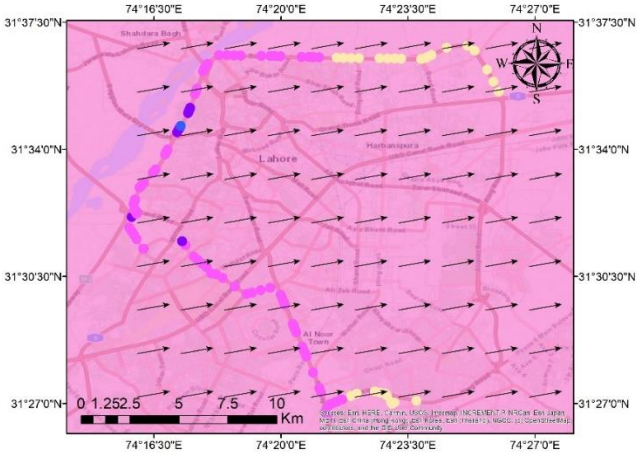

NO_2 Lahore 3rd November 2019

Round 2 (Wind speed 11 Km/h)

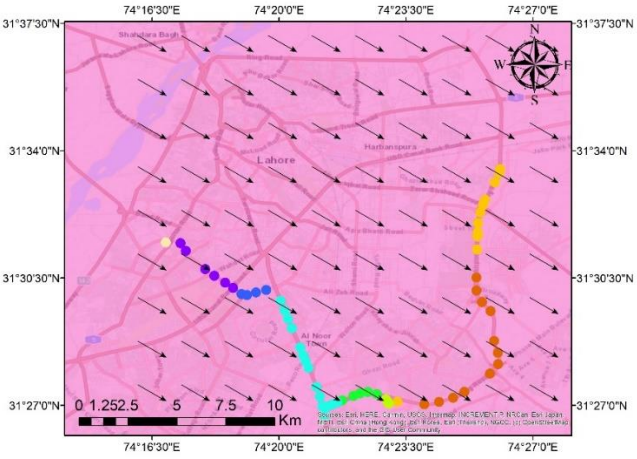

NO_2 Lahore 3rd December 2019

Round 1 (Wind speed 0 Km/h)

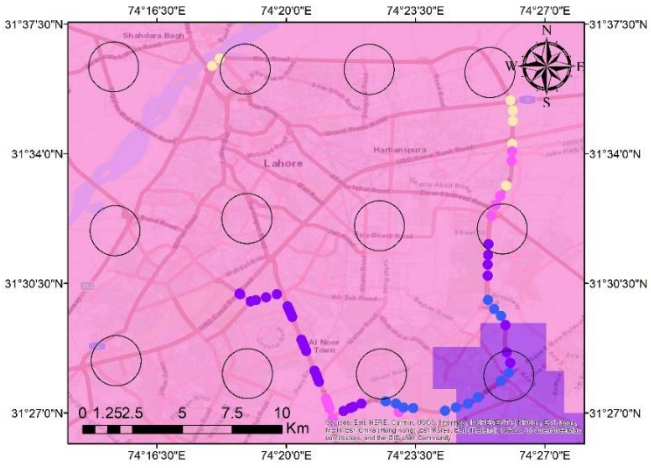

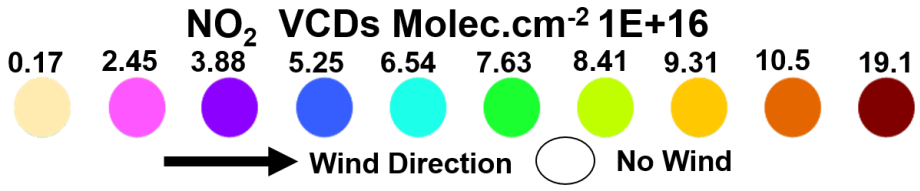

NO_2 Lahore 17th January 2020
Round 1 (Wind speed 0 km/h)

NO_2 Lahore 17th January 2020
Round 2 (Wind speed 0 Km/h)

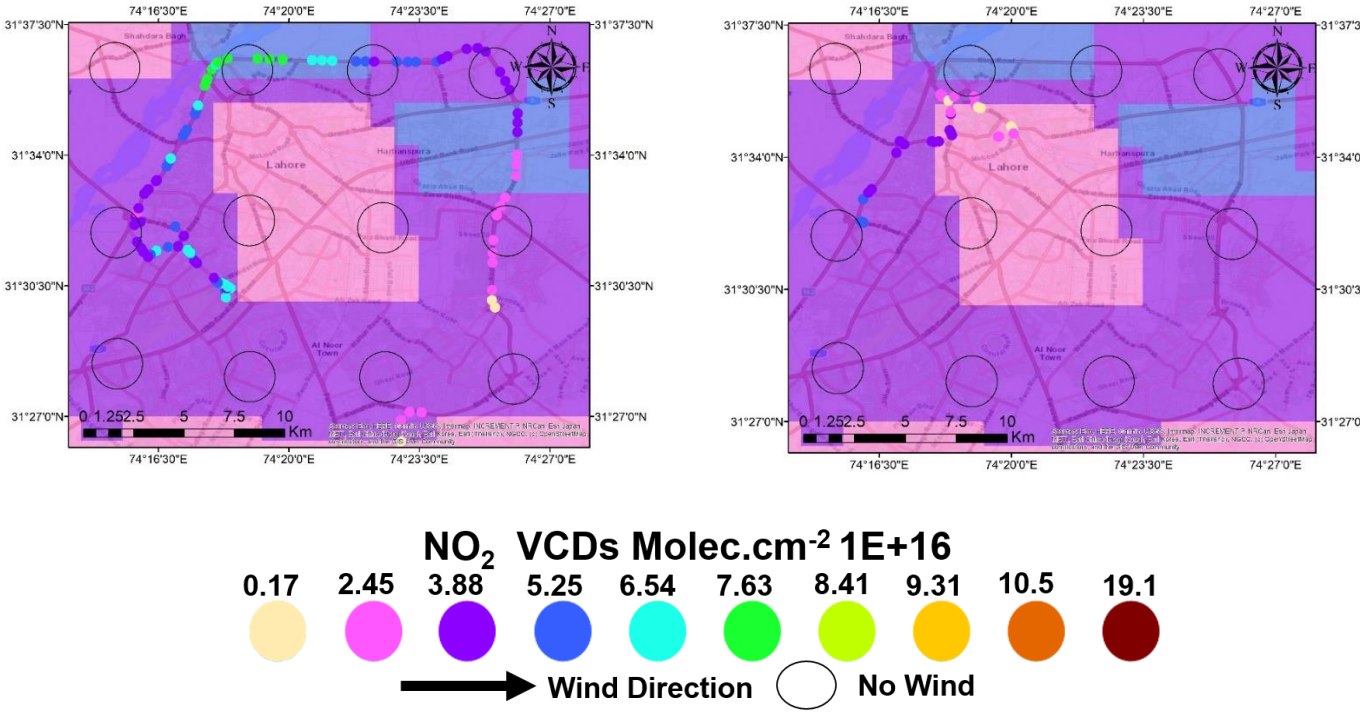

Figure 4.12: Results of MAXDOAS field campaigns conducted in Lahore (November 2019-December 2020).

Various field campaigns were also conducted around and inside Multan city, the results of these campaigns are presented in figure 4.14. The highest columns of NO_2 were observed on two sections of the Multan southern bypass, on 4 November 2019. The first section was from Ibn-Sina Hospital to Budhla Sant road, this section contained many smoke-spewing heavy vehicles like buses, trucks, and tractors. Another section of the southern bypass near Bahawalpur road showed high levels of NO_2, several heavy vehicles were also observed in this section as well traffic from the surrounding urban areas. The area near the center of the city near Altaf town close to Multan's airport showed some high levels most likely because of traffic. Higher columns were also observed near Khanewal road, these columns can be attributed to the nearby industries and traffic loads.

NO_2 Multan 4th November 2019
(Wind speed 7 Km/h)

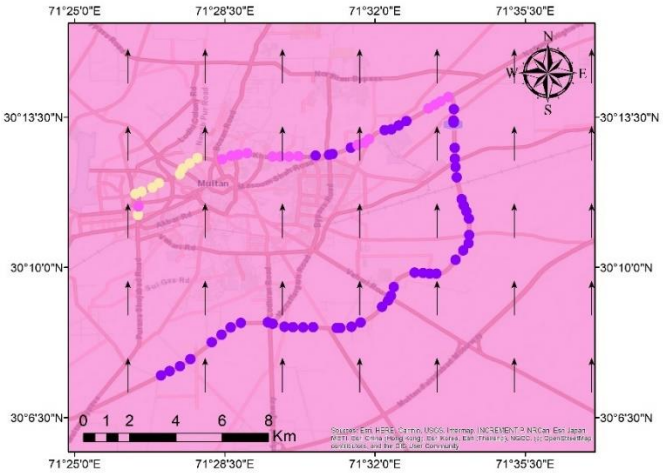

NO_2 Multan 4th December 2019
Round 1 (Wind speed 0 Km/h)

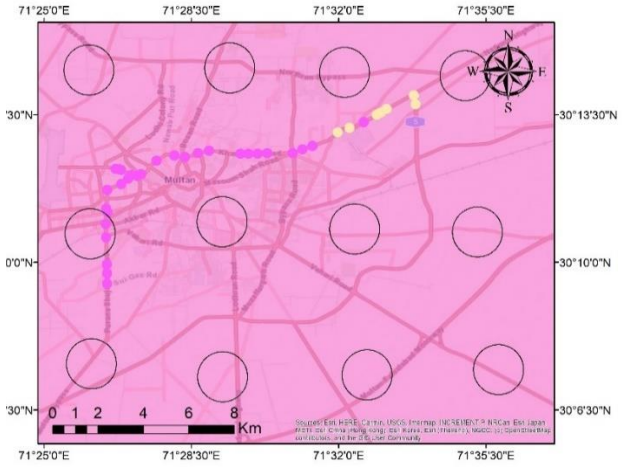

NO_2 Multan 4th December 2019
Round 2 (Wind speed 0 Km/h)

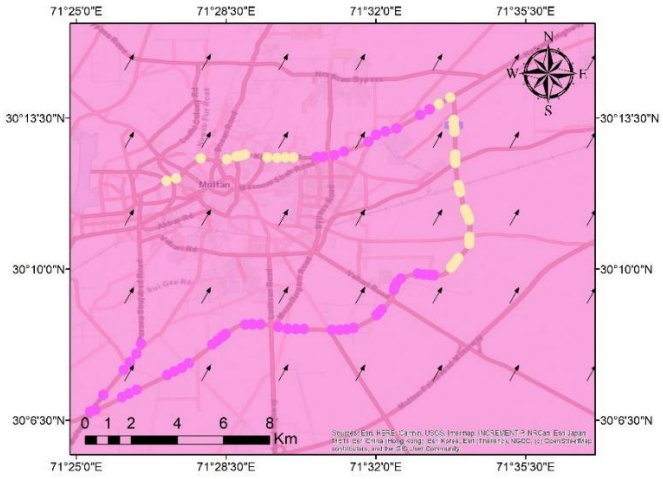

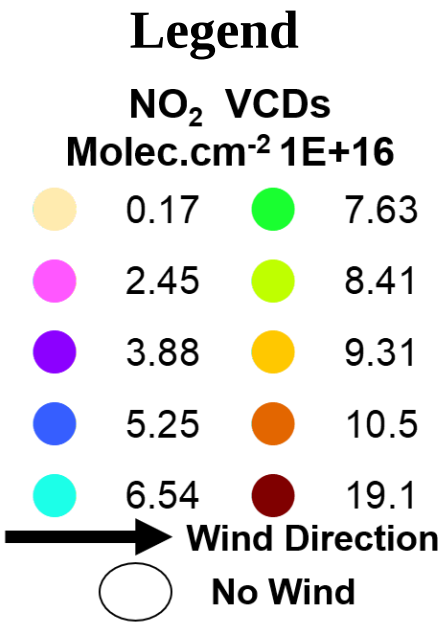

Figure 4.13: Results for MAXDOAS Field campaigns conducted in Multan (November 2019-January2020).

4.4.1. Analysis of the Criteria pollutants monitored in Lahore & Multan

Figure 4.14 represents the daily concentration of three criteria pollutants (CO, NOx, and O_3) measured at Lahore from October 2019 to February 2020 using the HAZ-Scanner instrument. The reddish lines represent the Pakistan Environmental Quality standards for these pollutants within ambient air converted into ppm and ppb (for 25oC temperature). According to figure 4.15, the concentration of both CO and O_3 are far below the PEQs while the concentrations of NOx

pollutants remains consistently above the standard prescribed limit for most of the winter months.

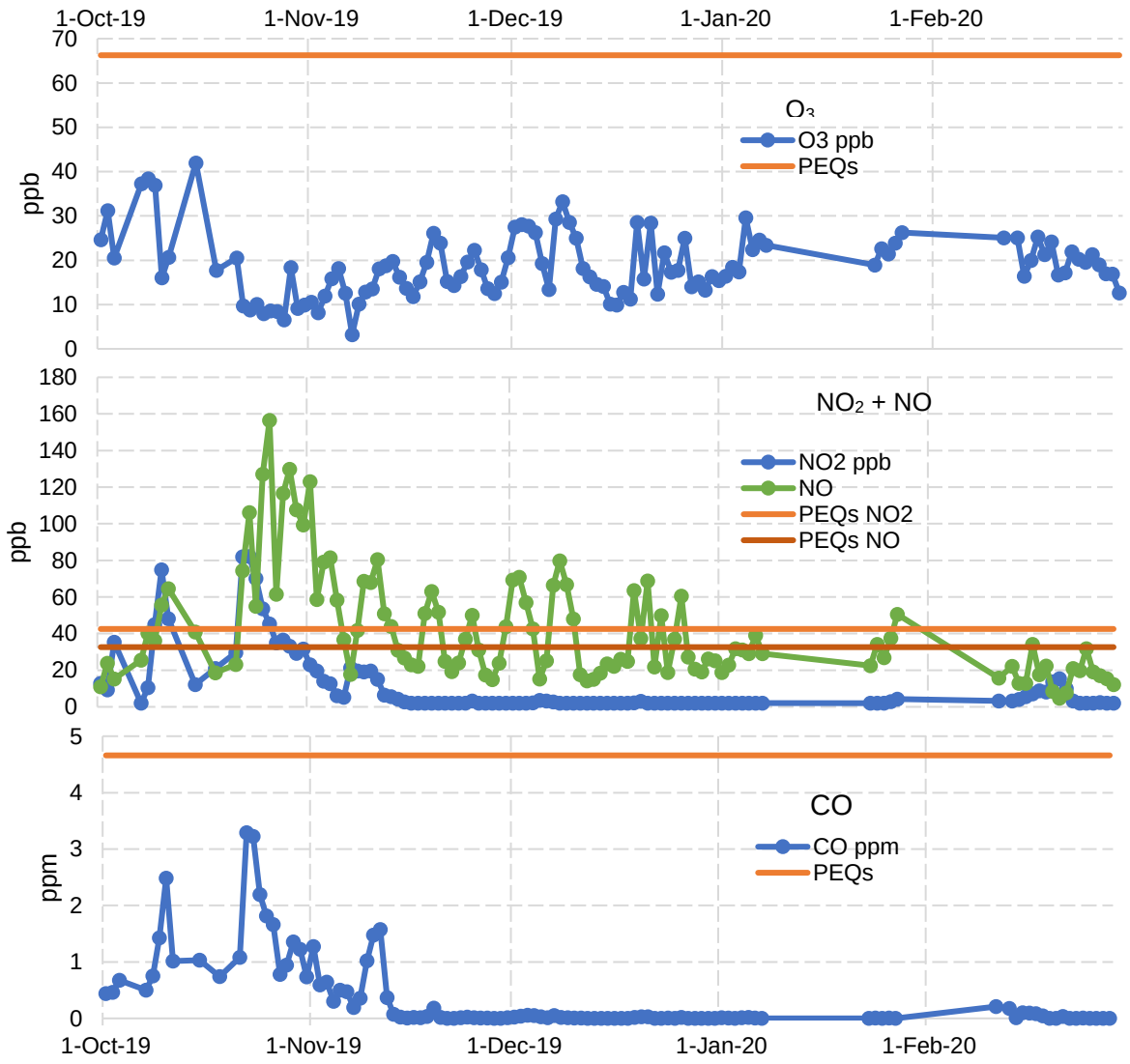

Figure 4. 14: Daily concentrations of O3, NO2, NO, and CO in Lahore from October 2019 to February 2020.

In figure 4.14 concentrations of O_3 exhibit an inverse relationship with NO and NO_2 i.e., a higher concentration of NOx was followed by lower concentrations of O_3 and vice versa. This could be a result of most of the O_3 in Lahore being produced by the breakdown of NOx as a secondary pollutant. These high concentrations of NOx and similar concentrations for CO could be the result of transportation and vehicular emissions as well as agricultural burning activities taking place around this period. Figure 4.16 represents the daily concentration of the criteria pollutants

CO and NOx (NO and NO_2) measured at Multan from October 2019 to January 2020 using the HAZ-Scanner instrument. The reddish lines represent the Pakistan Environmental Quality standards for these pollutants within ambient air converted into ppm and ppb (for 25°C temperature). According to this figure, the concentration of CO similar to Lahore remains below the PEQs while the concentrations of NOx remain above the standard prescribed limits during the post-monsoon and early winter periods.

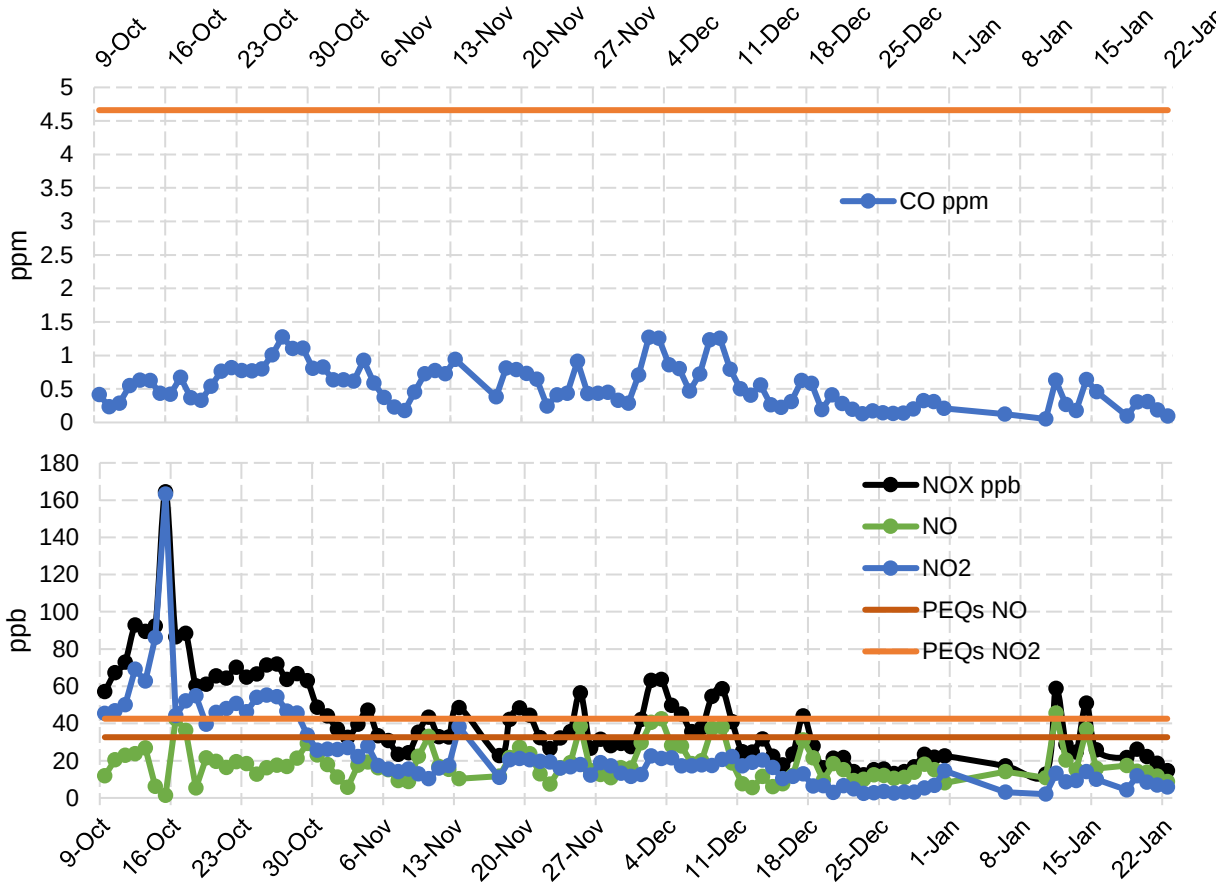

Figure 4.15: Daily concentrations of O3, NO2, NO, and CO in Multan from October 2019 to January 2020.

5.1.1. Trans-boundary effects from India in 2019

In this section, the possible trans-boundary effects of air pollution are assessed through a combination of ground-based field campaigns and back-trajectory simulations. As mentioned in the previous sections the highest agricultural burning activities across South-Asia (India and

Pakistan especially) are observed between 25-oct to 15-Nov, during this period MAX-DOAS based field campaigns were carried out across the city of Lahore. Back trajectory analysis was carried out in areas exposed to the highest air pollutant levels. In Figure 4.17, the highest values were noted near Shahdhra, where back trajectory analysis (from 3:00 pm local and 11:00 UTC) revealed that most of the air currents were being originated from the eastern sides of the international border, where a large number of fires and enhanced AOD levels were observed by the MODIS observation (31st Oct -1st November). This indicated that high values of air pollutants observed around the city of Lahore during car MAX-DOAS observations are most probably a result of local pollution sources coupled with trans-boundary pollution. However, in the absence of regular monitoring infrastructure in Lahore, estimating the total extent and potential damages associated with the trans-boundary pollution activities is difficult.

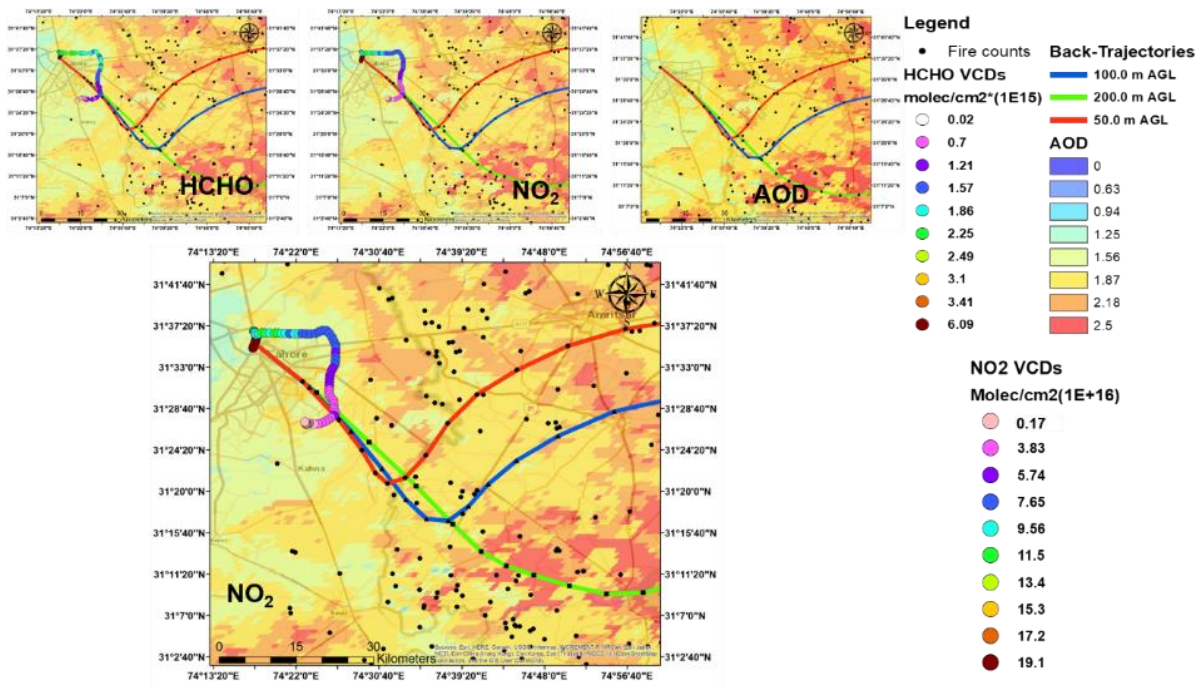

Figure 4.16: Trans-boundary effects of air pollution from India in 2019 estimated for NO2, CHOCHO, and HCHO columns observed in Lahore by exploiting car MAX-DOAS observations.

To assess the possible trans-boundary influences of the air masses a simple experiment was performed using the data obtained from the car-MAXDOAS field campaigns. The point where the highest values were observed for NO_2, HCHO, and CHOCHO was taken as the point of interest P2 (taken for 1st November around 3:00 pm) and back trajectories were calculated for this point by using the HYSPLIT trajectory model for the past 48 hours. These trajectories exhibited that air masses originating from India passing over the agricultural fire zones entered Lahore from the south and ended up at point P2. In the area where these air masses enter the path of the car-MAXDOAS campaign (referred to as P1), a spike in MAX-DOAS retrieved columns are visible at this point (a combination of background and trans-boundary pollutants). The point P0 is taken at a location without any industries or high traffic loads to represent the background values. Now the following equations are used to drive the trans-boundary and City plumes from this data.

P1 – P0 = Transboundary plume

P2 – P1 = City Plume

In the case of NO_2 columns (molecules/cm^2) these plumes were estimated to be around:

P1 – P0 = (5.74 – 0.01) E+16

P1 – P0 = 5.73 E+16 = Trans-boundary Contribution for NO_2 columns (30%)

P2 – P1 = (19.1 – 5.74) 1E+16

P2 – P1 = 13.36 E+16 = City Plume NO_2 (70%)

In the case of HCHO columns (molecules/cm^2), these plumes were estimated to be around:

P1 – P0 = (8.40 – 0.01) 1E+16

P1 – P0 = 8.39 E+16 = Trans-boundary Contribution for HCHO Columns (40%)

P2 – P1 = (21.0 – 8.40) 1E+16

P2 – P1 = 12.8 E+16 = City Plume HCHO (60 %)

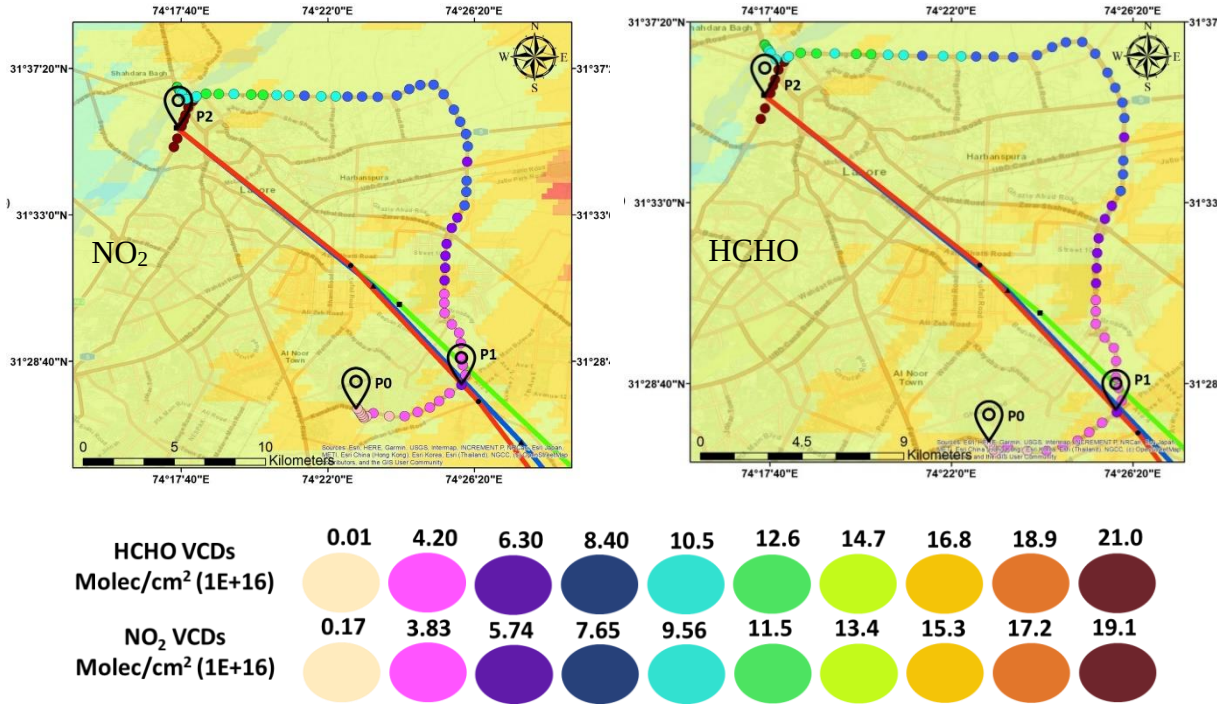

Figure 4. 3: Quantifying-Transboundary Pollution during MAXDOAS Field campaigns Lahore.

The results of the equation derived from MAX-DOAS field campaigns indicate that transboundary pollution does affect the air quality of Lahore to a certain extent. The observed effects of the trans-boundary loads coming from India and their contribution to NO_2 columns were low indicating that although NO_2 pollution does occur from trans-boundary pollution, in quantitative terms it is far less (30%) than the amount of NO_2 pollution generated from local sources (70%) such as transportation or industry. On the other hand, formaldehyde (HCHO) concentrations are more significantly affected by trans-boundary pollution activities (40%) taking place during this period, most likely because of its sensitivity to the large-scale agricultural fires occurring in India during this period. Although, the data from the field campaign conducted in Lahore during 1st November 2019 has facilitated with a quantitative assessment in the absence of standard air quality monitoring, however, one should be very careful while considering trans-boundary estimates for the following reasons:

i- these estimates are not precise enough to generalize for the whole time period, and relevant to that typical filed campaign only,

ii- ii- several other parameters like trajectory pathways, a lifetime of the target species, and role of meteorological parameters cannot be ruled out. Therefore, a more comprehensive study is required to completely understand the trans-boundary contribution to observed enhanced air pollution levels in Lahore or any other place.

1.1.1. Source Apportionment of various Air pollutants

Correlation matrix were created for the meteorological parameters (such as Temperature, Humidity, Wind speed) and pollution sources i.e. agricultural fires across south Asia (divided into local fires: Pakistan Punjab Fires, and transboundary fires: Indian fires) for the months of September to December (2015-2019). These matrices are represented in tables 4.1 to 4.14 below.

Table 4.1: Correlation matrix between AERONET AOD Lahore, Pakistan Punjab Fires and various meteorological Parameters

	AOD (A)	*Temp*	*Humidity (%)*	*W.S. m/s*	*Fires (P. Punjab)*
AOD (A)	100.00%				
Temp	4.13%	100.00%			
Hum (%)	38.57%	-39.68%	100.00%		
W.S. m/s	-6.01%	10.61%	-4.42%	100.00%	
Fires (P. Punjab)	-4.27%	-8.67%	-9.40%	-2.36%	100.00%

Table 2: Correlation matrix between MODIS AOD Lahore Indian Punjab Fires and various meteorological Parameters

	AOD (A)	*Temp*	*Humidity (%)*	*W.S. m/s*	*Fires (Indian Punjab)*
AOD (A)	100.00%				
Temp	4.13%	100.00%			
Hum (%)	38.57%	-39.68%	100.00%		
W.S. m/s	-6.01%	10.61%	-4.42%	100.00%	
Fires (Indian Punjab)	26.91%	11.72%	4.82%	-4.97%	100.00%

Table 4.3: Correlation matrix between MODIS AOD Lahore and Punjab Fires and various meteorological Parameters.

	AOD (M)	*Temp*	*Humidity (%)*	*W.S. m/s*	*Fires (P. Punjab)*
AOD (M)	100.00%				
Temp	0.84%	100.00%			
Hum (%)	44.95%	-39.68%	100.00%		
W.S. m/s	-7.79%	10.61%	-4.42%	100.00%	
Fires (P. Punjab)	-4.36%	-8.67%	-9.40%	-2.36%	100.00%

Table 4.4: Describes the correlation matrix between MODIS AOD Multan Pakistan Punjab Fires and various meteorological Parameters.

	AOD (Multan)	*Temp*	*Humidity (%)*	*W.S. m/s*	*Fires P.Punjab*
AOD (Multan)	100.00%				
Temp	-12.11%	100.00%			
Hum (%)	49.88%	-62.03%	100.00%		
W.S. m/s	-1.32%	28.05%	-22.44%	100.00%	

Fires P.Punjab	-7.46%	-4.62%	-13.96%	-8.47%	100.00%

It is clear from the correlation matrices created from the different parameters such as meteorology and pollution sources etc. That there is no significant correlation between meteorological parameters and other factors. However, we also know that correlation is not causation, it only informs us about the association among various factors through direct and indirect way. Several studies have described that air pollution and its complex interactions with meteorology cannot be adequately described through simple correlation (Fu et al., 2020; Jayamurugan et al., 2013; Kayes et al., 2019; Yin et al., 2016). To establish the linkage between these factors in the absence of correlation, we have utilized an alternative method known as Analytical Hierarchy Process (AHP). The results of the Analytical Hierarchy Process are described in table 4.7 and following criteria weightages have been associated with the major air pollutant sources during smog episodes. The consistency ratio for the study is also significantly below 0.10 showing good consistency in the matrix. According to the results, we can conclude that a large portion of the smog episodes is a result of transboundary pollution flowed by vehicular and thermal power generation sectors.

It is clear from the correlation matrices created from the different parameters such as meteorology and pollution sources etc. That there is no significant correlation between meteorological parameters and other factors. However, we also know that correlation is not causation, it only informs us about the association among various factors through direct and indirect way. Several studies have described that air pollution and its complex interactions with meteorology cannot be adequately described through simple correlation (Fu et al., 2020; Jayamurugan et al., 2013; Kayes et al., 2019; Yin et al., 2016). To establish the linkage between these factors in the absence of correlation, we have utilized an alternative method known as Analytical Hierarchy Process (AHP).

The analytical hierarchy process was conducted to estimate the most contributing factors to the annual smog episodes being quickly labeled as the "fifth season" in the country. According to the data assessed, the transboundary pollution resulting from open-burning activities in India Punjab has been assigned moderate importance over vehicular emissions, while strong and very strong importance over thermal power generation sources and brick kilns. Partly because of the low increase in thermal emissions over the previous years and the heavy restrictions imposed on brick kilns during the smog seasons, especially in red-zones categories like Lahore. The results of the AHP have been associated with the major air pollutant sources during smog episodes and are described below in Tables 4.5 to 4.6, where the greatest weightage is assigned to trans-boundary open burning, followed by vehicular emissions, followed by thermal or industrial emission, and then brick kilns. The consistency ratio for the study is also significantly below 0.10 showing good consistency in the matrix. According to the results presented in table 4.7, we can conclude that a large portion of the smog episodes is a result of trans-boundary pollution flowed by vehicular and thermal power generation sectors.

Table 4.5: Describes the pair-wise matrix based on relevance to smog episodes

	Transboundary	Vehicles	Thermal Power	Brick kilns
Transboundary	1.00	3.00	5.00	7.00
Vehicles	0.33	1.00	3.00	5.00
Thermal Power	0.20	0.33	1.00	3.00
Brick kilns	0.14	0.20	0.33	1.00

Where 1 = Same importance, 3 = Moderate importance, 5 = Strong importance, 7 = Very strong importance.

Table 4.6: Describes the normalized pair-wise matrix created from Table 4.5

Normalized Pairwise Matrix				
	Transboundary	**Vehicles**	**Thermal Power**	**Brick kilns**
Transboundary	0.60	0.66	0.54	0.44
Vehicles	0.20	0.22	0.32	0.31
Thermal Power	0.12	0.07	0.11	0.19
Brick kilns	0.09	0.04	0.04	0.06

Table 4.7: Describes the Criteria Weightage, λ Max, and consistency ratio for the AHP process

Pollution Sources	**Criteria Weight**	**λMax**	**Consistency ratio**
Transboundary	0.56	4.118466	0.039489
Vehicles	0.26		
Thermal Power	0.12		
Brick kilns	0.06		

Chapter 5

5. CONCLUSION AND RECOMMENDATIONS:

2.1. Conclusion

According to the results of the various monitoring activities carried across various cities of Pakistan, it was found that concentration of various pollutants in the cities were rising. Concentration of NO_2 consistently exceeds NEQs in Lahore and Multan and pollutant concentrations are largely governed by meteorological parameters and pollution sources. Amongst which transportation and industry stand out in Lahore.

Following are the conclusions drawn from the study:

- NO_2 columns observed with satellite instruments (OMI and TROPOMI) compared well with ground-based MAX-DOAS and exhibited similar temporal trends and strong correlation ranging from 0.77 to 0.91 among all data sets. However, satellite observations underestimate ground measurements significantly.

- Higher columns of NO_2 are observed during winter periods and lower concentration around summer and monsoon periods. Primarily, due to the role of stable atmospheric boundary layer conditions and use of extra sources for space heating.

- Fire activities including both local and transboundary play an important role in determining the air quality of various cities in Punjab Pakistan. The contribution is most prominent during the post -monsoon period with frequent and extensive smog episodes.

2.2. Recommendations

Following recommendations are based on the findings of this study with main emphasis on combating air pollution and improving the air quality in the country.

1. As large part of air pollution is being contributed from vehicular emissions, effective pollution control techniques such as alternative fuels, improved combustion technologies and catalytic converters is highly encouraged.

2. The use of mass transport systems in crowded urban areas is also recommended to avoid unnecessary congestion and traffic jams.

3. Effective media campaigns for educating the general public and other stakeholders, to improve their understanding and raising air quality concerns.

4. Pakistan's air quality management lacks the effective air quality monitoring network. Setting up proper air quality monitoring stations around major cities of the country and incorporating early warning and management approaches is recommended.

5. The establishment of an emission inventories and baseline studies for various cities in Pakistan is strongly recommended.